

Tricyclic indazoles – a novel class of selective estrogen receptor degrader antagonists.

James S. Scott, Andrew Bailey, David Buttar, Rodrigo J. Carbajo, Jon Curwen, Paul Davey, Robert D. M. Davies, Sebastien L. Degorce, Craig Donald, Eric Gangl, Ryan David Robert Greenwood, Sam Groombridge, Tony Johnson, Scott Lamont, Mandy Lawson, Andrew Lister, Christopher Morrow, Thomas A. Moss, Jennifer H Pink, and Radoslaw Polanski

J. Med. Chem., **Just Accepted Manuscript** • DOI: 10.1021/acs.jmedchem.8b01837 • Publication Date (Web): 14 Jan 2019

Downloaded from <http://pubs.acs.org> on January 14, 2019

Just Accepted

“Just Accepted” manuscripts have been peer-reviewed and accepted for publication. They are posted online prior to technical editing, formatting for publication and author proofing. The American Chemical Society provides “Just Accepted” as a service to the research community to expedite the dissemination of scientific material as soon as possible after acceptance. “Just Accepted” manuscripts appear in full in PDF format accompanied by an HTML abstract. “Just Accepted” manuscripts have been fully peer reviewed, but should not be considered the official version of record. They are citable by the Digital Object Identifier (DOI®). “Just Accepted” is an optional service offered to authors. Therefore, the “Just Accepted” Web site may not include all articles that will be published in the journal. After a manuscript is technically edited and formatted, it will be removed from the “Just Accepted” Web site and published as an ASAP article. Note that technical editing may introduce minor changes to the manuscript text and/or graphics which could affect content, and all legal disclaimers and ethical guidelines that apply to the journal pertain. ACS cannot be held responsible for errors or consequences arising from the use of information contained in these “Just Accepted” manuscripts.

Tricyclic indazoles – a novel class of selective estrogen receptor degrader antagonists.

James S. Scott, Andrew Bailey,* David Buttar,* Rodrigo J. Carbajo,* Jon Curwen,* Paul R. J. Davey,* Robert D. M. Davies,* Sébastien L. Degorce,* Craig Donald,* Eric Gangl,♦ Ryan Greenwood,* Sam D. Groombridge,* Tony Johnson,* Scott Lamont,* Mandy Lawson,* Andrew Lister,* Christopher J. Morrow,* Thomas A. Moss,* Jennifer H. Pink,* Radoslaw Polanski.♥*

* Oncology, IMED Biotech Unit, AstraZeneca, Cambridge CB4 0WG, United Kingdom.

♦ Oncology IMED Biotech Unit, AstraZeneca, R&D Boston, 35 Gatehouse Drive, Waltham, Massachusetts 02451, United States.

♥ Discovery Sciences, IMED Biotech Unit, AstraZeneca, Cambridge CB4 0WG, United Kingdom.

ABSTRACT

Herein we report the identification and synthesis of a series of tricyclic indazoles as a novel class of selective estrogen receptor degrader antagonists. Replacement of a phenol, present in our previously reported tetrahydroisoquinoline scaffold, with an indazole group led to removal of a reactive metabolite signal in a *in vitro* glutathione trapping assay. Further optimization, guided

1
2 by X-ray crystal structures and NMR conformational work, varied the alkyl sidechain and
3
4
5 pendant aryl group and resulted in compounds with low turnover in human hepatocytes and
6
7
8 enhanced chemical stability. Compound **9** was profiled as a representative of the series in terms
9
10
11
12 of pharmacology and demonstrated the desired ER α degrader-antagonist profile and
13
14
15
16 demonstrated activity in a xenograft model of breast cancer.
17
18
19
20
21
22

23 INTRODUCTION

24
25 Breast cancer is the second most common type of cancer and the most frequently occurring cancer
26
27 amongst women, with an estimated 1.67 million new cancer cases diagnosed in 2012, constituting 25% of
28
29 all cancers.¹ In 2012 in the US it is estimated that 233,000 women were diagnosed with breast cancer and
30
31 44,000 women died from the disease; in the same year in the European Union an estimated 367,000
32
33 women were diagnosed with breast cancer and 91,000 died from the disease.¹ Approximately 80% of
34
35 post-menopausal women with breast cancer have estrogen receptor α (ER α)-positive disease.²
36
37
38
39
40

41 In patients with ER α -positive breast cancer, endocrine therapies such as tamoxifen and aromatase
42
43 inhibitors (AI) have been the mainstay treatment. However, advanced breast cancer remains incurable,
44
45 with patients ultimately relapsing due to acquired or *de novo* resistance. Numerous resistance
46
47 mechanisms to anti-estrogens have been suggested. These include mutations in ER α that lead to ligand-
48
49 independent activation,³ activation of signaling pathways that can cause ER α activation in the absence of
50
51 estradiol⁴ and changes in expression of ER α -cofactors which result in ER α modulators, such as
52
53
54
55
56
57
58
59 tamoxifen, becoming agonists.⁴ In all these cases, ER α activity is still required. This continual
60

1 dependence of tumours on ER α highlights a currently unmet medical need to achieve a more complete
2 inhibition of the pathway.
3
4
5

6
7 Fulvestrant is a selective estrogen receptor degrader (SERD) which has demonstrated superiority over the
8 aromatase inhibitor, anastrozole.⁵ Introduced into clinical practice in 2002, fulvestrant is an ER α
9 antagonist with no known confounding agonist properties and has the unique ability to increase the rate of
10 turnover of the receptor which limits the amount available for potential further activation. This has led to
11 a focus on SERDs as a strategy for inhibition and removal of ER α . However, the use of fulvestrant is
12 limited in the clinic by a lack of oral bioavailability and is administered intramuscularly in doses of 500
13 mg once a month which could limit clinical efficacy.⁵ Oral SERDs could potentially achieve higher free
14 drug levels than has been possible with fulvestrant and this, in turn, might lead to a more complete
15 removal of ER α and a more durable response in patients.
16
17
18
19
20
21
22
23
24
25
26
27
28
29
30
31

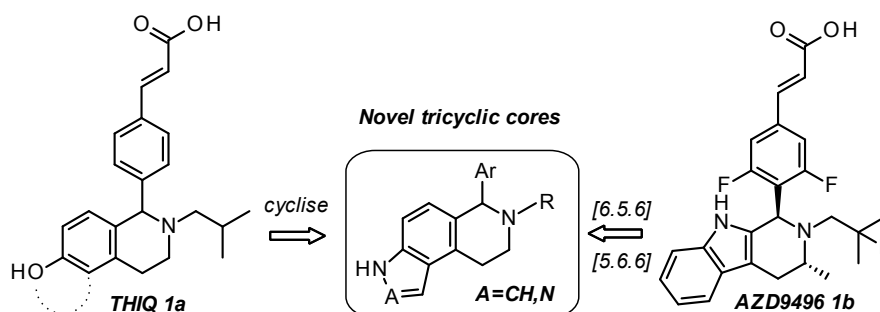
32 Given the importance of ER α as an oncology target, considerable effort has been devoted to identifying
33 an orally bioavailable SERD. A number of promising SERD compounds featuring a phenyl substituted
34 acrylic acid motif have been described recently. Initially reported on a triarylethylene scaffold GW7604⁶
35 this group also appears in the development candidates GDC-810⁷ from Seragon/Genentech, AZD9496⁸
36 **1b** from AstraZeneca and LSZ102⁹ from Novartis. Other scaffolds containing the phenyl substituted
37 acrylic acid have been reported by AstraZeneca (coumarin¹⁰ and tetrahydroisoquinoline¹¹), GSK
38 (quinoline¹²) and Novartis (tetrahydroisoquinoline¹³) as well as the Trinity Biomedical Sciences Institute
39 (benzoxepin¹⁴), the State University of New York at Stony Brook, (coumarin¹⁵ and triarylethylene¹⁶), the
40 University of Illinois at Chicago (benzothiophene¹⁷) and the University of Illinois at Urbana–Champaign
41 (bicyclononane¹⁸ and adamantyl¹⁹). With the notable exceptions of **1b** and GDC-810, the key compounds
42 described in each case relied on a phenol for potency. Recent work from the RCMI Cancer Research
43 Center has shown that a boronic acid can act as a surrogate for the phenol on a triarylethylene scaffold,
44 leading to GLL398.²⁰
45
46
47
48
49
50
51
52
53
54
55
56
57
58
59
60

Other SERDs have entered clinical development such as RAD1901²¹ from Radius and GDC-927²² from Seragon/Genentech which have basic groups showing that groups other than the acyclic acid are capable of giving a SERD phenotype.

RESULTS AND DISCUSSION

We previously reported a series of tetrahydroisoquinoline (THIQ) phenols that showed an ER degrader-antagonist profile.¹¹ These compounds were observed to trap glutathione (GSH) in an *in vitro* microsome based trapping assay,²³ potentially indicative of a reactive metabolite risk. The GSH trapping was shown to be attributable to the phenol functionality but the phenol was also demonstrated to be critical for potency. We were thus drawn to investigate potential phenol replacements and targeted tricyclic indole and indazole cores that had not been previously described in the chemical literature.²⁴ We were intrigued to explore whether these cores might be able to mimic the interaction with the salt bridge exploited by the phenol by providing a suitably oriented hydrogen bond donor. In viewing the indole as a structural isomer of the core present in **1b**, we hypothesized that the alteration in connectivity of the ring system from a [6.5.6] to a [5.6.6] system (Figure 1.) might switch the interaction made by the respective indole NH's from a backbone carbonyl to the salt bridge.

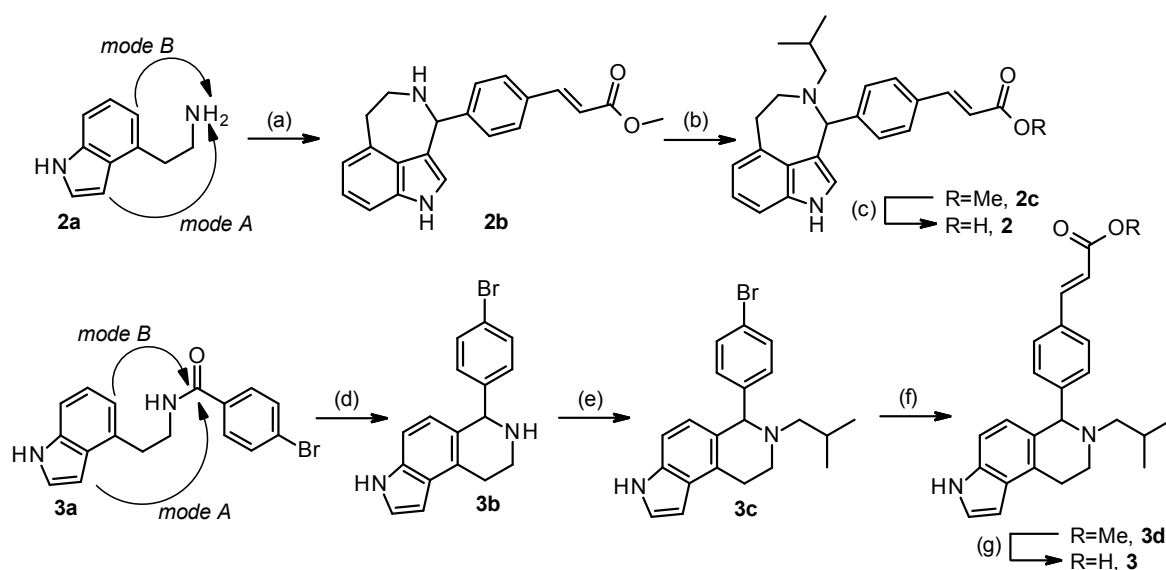
Figure 1. Core designs based on hybridization of THIQ and tricyclic indole equity



Synthesis of compounds

We therefore developed chemical routes towards these motifs as shown in Schemes (1-7). Our initial attempts to synthesize the tricyclic indole core involved a Pictet-Spengler cyclization between indole amine **2a** and (*E*)-methyl 3-(4-formylphenyl)acrylate. Unfortunately, the major product from this reaction was the unusual [5.6.7]-fused tricyclic amine **2b** where the cyclization had occurred *via* the C3 position of the indole ring (mode A) in preference to the desired reaction through the phenyl ring (mode B).²⁵ This was subsequently alkylated and deprotected to give **2** (Scheme 1). In order to access the targeted tricyclic core, we resorted to a Bischler-Napieralski approach with the cyclization of amide **3a** followed by reduction of the imine intermediate to give a 33% yield of the desired cyclization product **3b** (*via* mode B). Subsequent alkylation to give **3c** was followed by a Heck reaction to introduce the acrylate group **3d** and ester hydrolysis to give **3**.

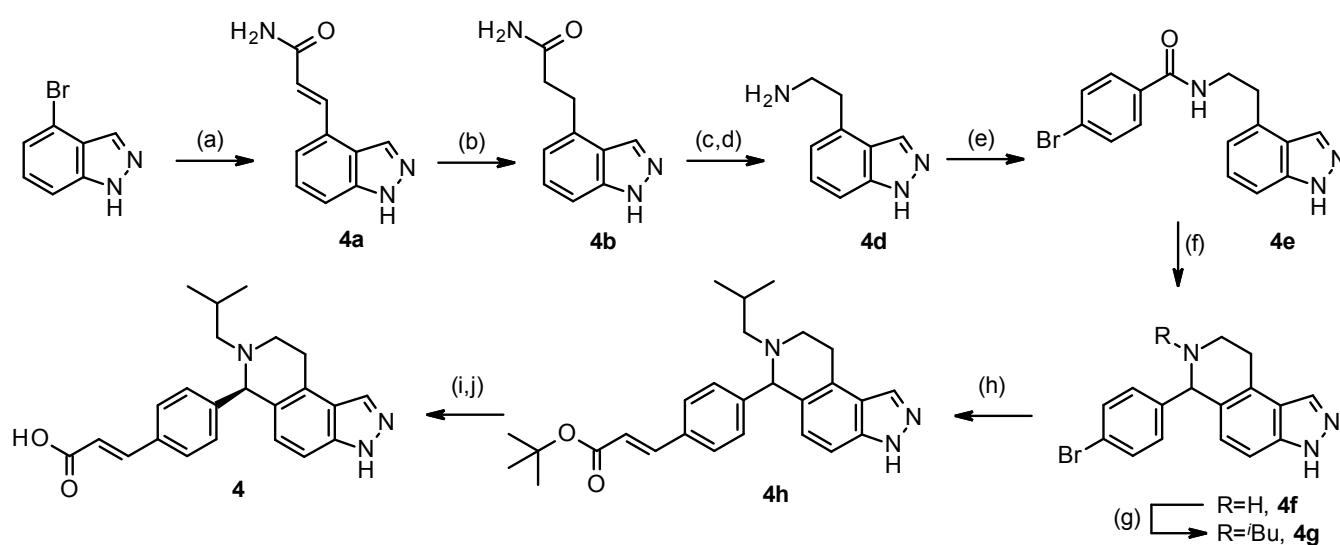
Scheme 1. Pictet-Spengler and Bischler-Napieralski approaches to tricyclic indole^a



^aReagents and Conditions: (a) (*E*)-methyl 3-(4-formylphenyl)acrylate, AcOH, toluene, 80 °C, 2 h, 31%; (b) isobutyl trifluoromethanesulfonate, DIPEA, 1,4-dioxane, RT, 4 d, 72%; (c) NaOH, THF/MeOH, RT, 24 h, 86%; (d) POCl₃, 110 °C, 3 h, then NaBH₄, MeOH, 0 °C, 16 h 33%; (e) isobutyl trifluoromethanesulfonate, DIPEA, 1,4-dioxane, RT, 24 h, 67%; (f) methyl acrylate, NMeCy₂, Pd-118, TBAC, MeCN, 150 °C, 1 h, 63%; (g) NaOH, THF/MeOH, RT, 24 h, 61%.

1
2 Indazole **4** was synthesized racemically from commercially available 4-bromo-1*H*-indazole. Heck
3
4
5
6 reaction with acrylamide gave the alkene **4a**, which was hydrogenated with Pd/C to give
7
8
9 saturated amide **4b**. Curtius rearrangement followed by Boc deprotection gave the amine **4d**,
10
11
12 which was reacted with 4-bromobenzoic acid and HATU to afford the amide **4e**. Bischler-
13
14
15 Napieralski cyclization, followed by reduction of the imine with NaBH₄ gave the tricyclic indazole
16
17
18 **4f**, which was alkylated *via* reductive amination to give **4g**. A Heck reaction on the bromide with
19
20
21
22 *tert*-butylacrylate gave ester **4h**, and subsequent hydrolysis of the *tert*-butyl ester afforded the
23
24
25
26
27
28
29
30
31
32
33
34
35
36
37
38
39
40
41
42
43
44
45
46
47
48
49
50
51
52
53
54
55
56
57
58
59
60
racemic acid which was separated by chiral chromatography into enantiomerically pure **4**
(Scheme 2).

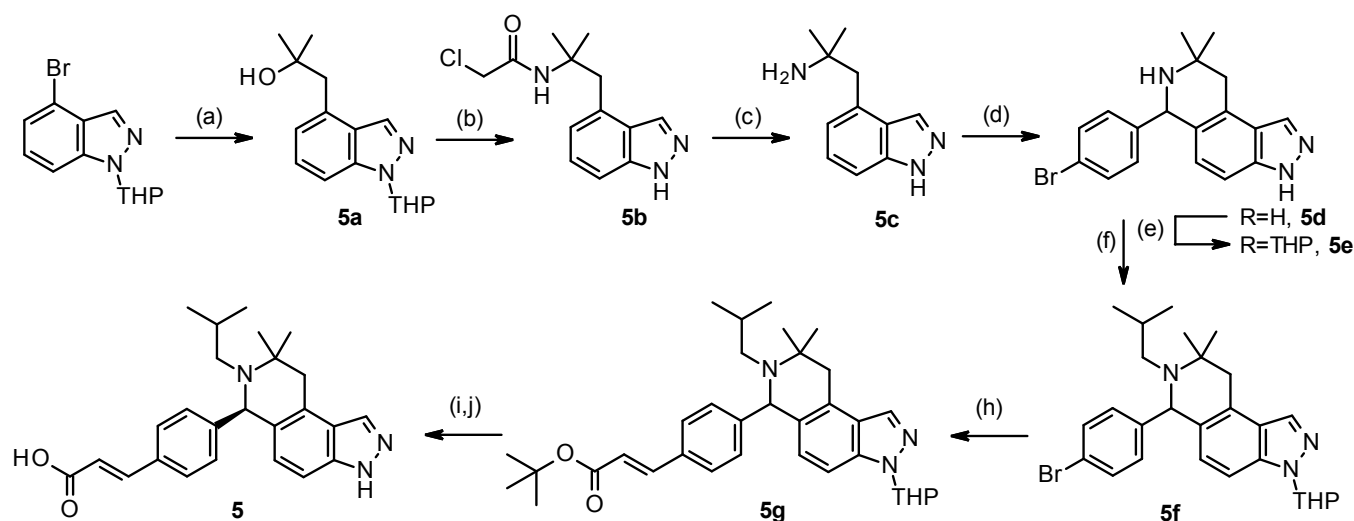
Scheme 2. Bischler-Napieralski route to tricyclic indazole^a



1
2 ^aReagents and Conditions: (a) acrylamide, NMeCy₂, Pd-118, TBAC, MeCN, 130 °C, 2 h, 41%; (b) Pd/C,
3
4 H₂, EtOH, RT, 23 h, 94%; (c) Pb(OAc)₄, ^tBuOH, 80 °C, 45 min, 67%; (d) TFA, DCM, RT, 1 h, 93%; (e)
5
6 4-bromobenzoic acid, HATU, DIPEA, DMF, RT, 1 h, 73%; (f) POCl₃, P₂O₅, reflux, 9 h, then NaBH₄,
7
8 MeOH, THF, RT, 1 h, 77%; (g) isobutyrylaldehyde, Na(OAc)₃BH, AcOH, DCE, NMP, RT, 1 h, 93%; (h)
9
10 *tert*-butyl acrylate, NMeCy₂, Pd-118, TBAC, MeCN, 150 °C, 45 min, 77%; (i) DCM, TFA, RT, 45 min;
11
12
13 (j) chiral separation, 38% over 2 steps.
14
15
16
17
18
19

20 Introduction of *geminal*-dimethyl substitution into the saturated ring could be achieved from the
21
22 THP-protected 4-bromo-indazole. Lithium-halogen exchange with *n*-BuLi followed by quenching
23
24 with dimethyloxirane and BF₃.Et₂O afford the tertiary alcohol **5a**. Ritter reaction with
25
26 chloroacetonitrile, followed by cleavage of the amide of **5b** with thiourea furnished the *gem*-
27
28 dimethyl amine **5c**. The saturated ring of **5d** was then constructed with a Pictet-Spengler
29
30 cyclization using 4-bromobenzaldehyde. In this case, the imine was pre-formed using pH 6
31
32 phosphate buffer, before heating in TFA to effect cyclization. THP protection of the indazole
33
34 gave **5e** then alkylation with isobutyl triflate and DIPEA afforded **5f**. Subsequent Heck reaction
35
36 installed the acrylic ester to give **5g**, which was hydrolyzed under acidic conditions with
37
38 concomitant deprotection of the THP group. A final chiral separation of the enantiomers
39
40
41
42
43
44
45
46
47
48
49
50
51
52
53
54
55
56
57
58
59
60 afforded enantiopure **5** (Scheme 3).

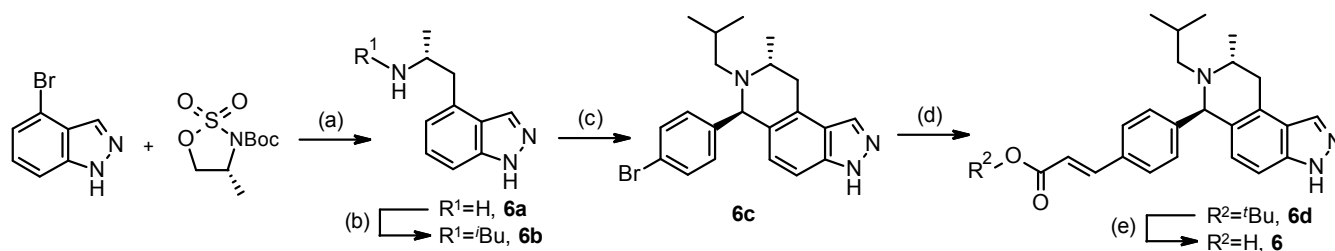
Scheme 3. Pictet-Spengler route to *gem*-dimethyl substituted tricyclic indazole^a



^aReagents and Conditions: (a) *n*-BuLi, 2,2-dimethyloxirane, BF₃·Et₂O, THF, -78 °C, 1 h, 62%; (b) 2-chloroacetonitrile, AcOH, H₂SO₄, RT, 48 h, 59%; (c) thiourea, EtOH, AcOH, Δ, 16 h, 83%; (d) potassium phosphate buffer (0.1M, pH 6), MeCN, 50 °C, 16 h, then TFA, 130 °C, 5 h, 51%; (e) 3,4-dihydro-2H-pyran, PTSA hydrate, DCM, 40 °C, 16 h; (f) isobutyl trifluoromethanesulfonate, DIPEA, dioxane, RT, 24 h, 22% over 2 steps; (g) *tert*-butyl acrylate, NMeCy₂, Pd-118, TBAC, MeCN, 150 °C, 1 h, 89%; (h) TFA, DCM, RT, 2 h; (i) chiral chromatography, 35% over 2 steps.

Incorporation of a single methyl substituent on the saturated ring provided a significant synthetic challenge. Traditional Bischler-Napieralski or Pictet-Spengler cyclizations where the amine was unalkylated afforded the undesired *cis*-isomer as the major product.²⁶ A *trans* relationship between methyl and aryl substituents could be achieved in low yield *via* Pictet-Spengler cyclization of alkylated tryptamine **6b** which was synthesized by ring opening of a chiral cyclic sulfamidate to give **6a**, followed by reductive amination with isobutyraldehyde.²⁷ This established a chiral relay where the chirality of the methyl group established the *trans*-relationship and controlled the absolute stereochemistry of the newly formed chiral centre. However, the harsh conditions required meant that only robust alkyl sidechains such as *i*Bu were tolerated. Heck reaction on the Pictet-Spengler product **6c**, followed by hydrolysis of the *tert*-butyl ester of **6d** afforded the desired acrylic acid **6** (Scheme 4).

Scheme 4. Pictet-Spengler route to 1,3-*trans* methyl substituted tricyclic indazole^a

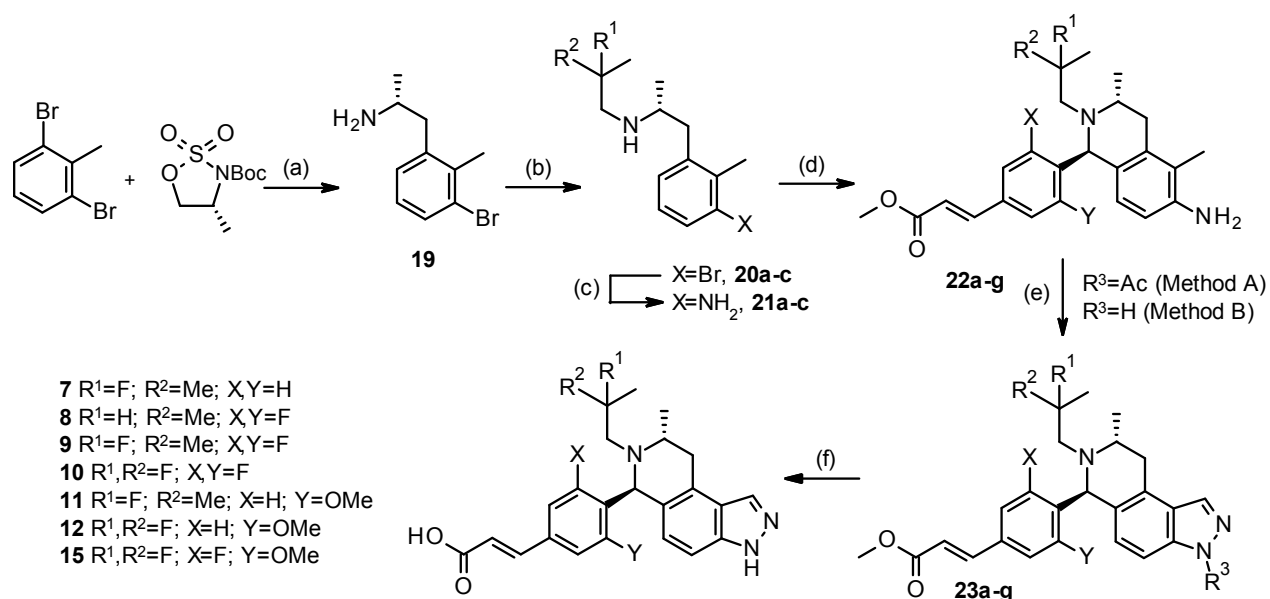


^aReagents and Conditions: (a) *n*-BuLi, THF, -78 °C to 0 °C, 1 h, 78% then 4N HCl/dioxane, RT, 1 h, 87%; (b) isobutyrylaldehyde, Na(OAc)₃BH, THF, 5 °C, 30 min, 80%; (c) 4-bromobenzaldehyde, TFA, toluene, 150 °C, 40 h, 14%; (d) *tert*-butyl acrylate, NMeCy₂, Pd-118, TBAC, MeCN, 150 °C, 45 min, 80%; (e) TFA, DCM, RT, 45 min, 19%.

To achieve variation of the *N*-alkyl sidechain and aryl ring, a more flexible approach was developed that was tolerant to a range of functionality. This involved performing the Pictet-Spengler cyclization on an aniline substrate and subsequently constructing the indazole ring. Treatment of 2,6-dibromotoluene with *n*-BuLi in THF at -78 °C, followed by addition of cyclic sulfamidate gave the aliphatic amine **19** after Boc deprotection. *N*-Alkylation could be achieved by heating this amine with the requisite alkyl triflate and DIPEA in 1,4-dioxane to give **20a-c**. Buchwald amination with benzophenone imine, followed by hydrolysis with aqueous acid afforded the anilines **21a-c**. The anilines were then subjected to Pictet-Spengler cyclization with aldehydes already bearing the acrylic ester to furnish the cyclized products **22a-g** as the desired *trans* isomers. Interestingly, this cyclization proceeded more smoothly with a small amount of

water present in the AcOH; it was hypothesized that the water helps to hydrolyse the imine formed from condensation of the aniline with the aldehyde, allowing cyclization to occur. Indazole formation could then be achieved by either heating the aniline with isopentyl nitrite and acetic anhydride under basic conditions ('Method A'), or with NaNO₂ in a mixture of propionic acid and water under cooling ('Method B'). Hydrolysis of the acrylic esters (and *N*-acetyl where Method A was used) afforded the acrylic acids **7-12** and **15** (Scheme 5).

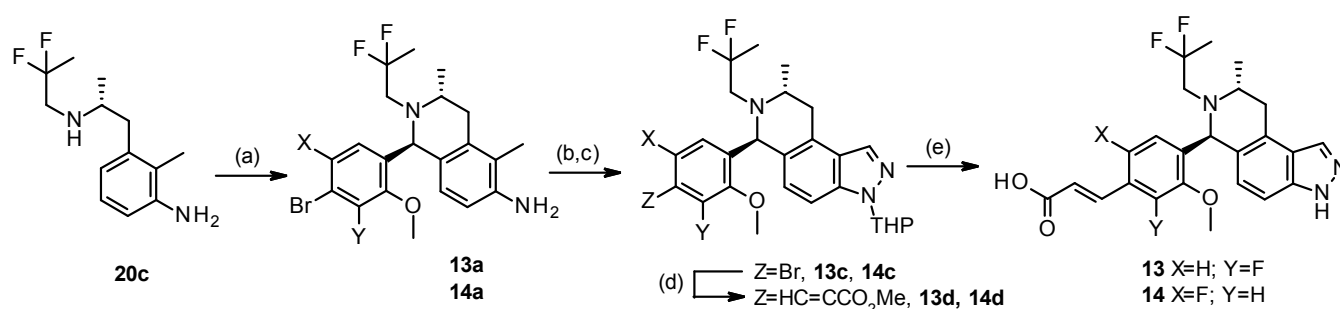
Scheme 5. 2nd generation route with late stage indazole formation.



^aReagents and Conditions: (a) *n*-BuLi, THF, -78 °C to 0 °C, 1 h, then 4N HCl/dioxane, RT, 1 h, 61%; (b) alkyl triflate, DIPEA, 1,4-dioxane, 90 °C, 66-74% or isobutyrylaldehyde, Na(OAc)₃BH, THF, 0 °C, 56%; (c) benzophenone imine, Pd₂dba₃, Rac-BINAP, NaO^tBu, toluene, 90 °C, then 1N aq. HCl, 71-91%; (d) aldehyde, AcOH (1% H₂O), 60-100 °C, 30-57%; (e) *Method A*: isopentyl nitrite, Ac₂O, KOAc, 18-crown-6, chloroform, 70 °C, 48 h, or *Method B*: NaNO₂, propionic acid, water, -10 °C, 1 h; (f) *Method A* and *Method B*: aq. NaOH, THF, MeOH, RT-60 °C, 1-16 h, 65-96%.

Further variation in the pendant phenyl ring was achieved *via* a closely related route. In this case, the Pictet-Spengler cyclization was carried out on aldehydes containing a 4-bromo substituent. Following construction of the indazole ring, this was used to introduce the acrylic acid using a Heck reaction on methyl acrylate followed by hydrolysis of the ester (Scheme 6).

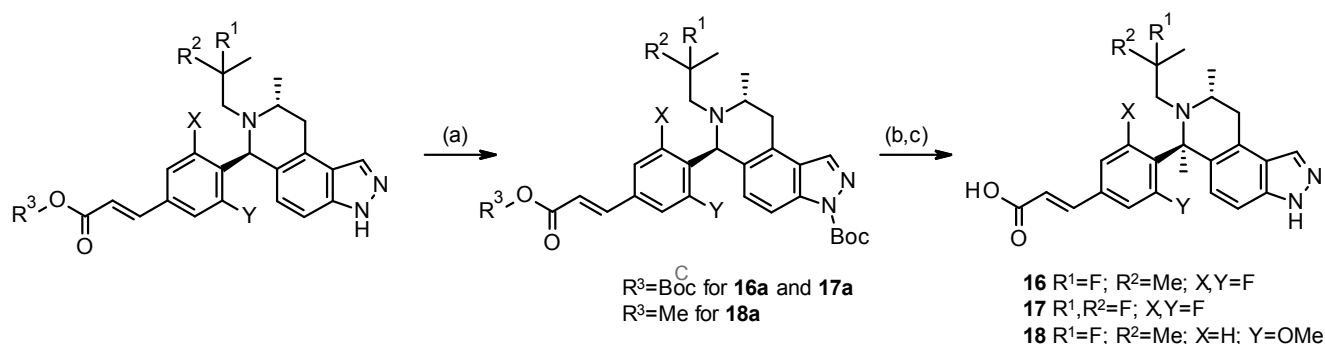
Scheme 6. Variation of the pendant phenyl ring^a



^aReagents and Conditions: (a) aldehyde, AcOH (1% H₂O), 90 °C, 16 h, 50% for **13a**, 26% for **14a**; (b) NaNO₂, propionic acid, H₂O, -20 °C, 45-60 min, 70% for **13b**, 92% for **14b**; (c) 3,4-dihydro-2*H*-pyran, PTSA hydrate, DCM, reflux, 3 h, 95% for **13c**, 93% for **14c**; (d) methyl acrylate, Pd-118, DIPEA, 1,4-dioxane, 125 °C, 2 h, 63% for **13d**, 53% for **14d**; (e) 4N HCl dioxane, RT, 15-30 min, then LiOH.H₂O, THF/MeOH/ H₂O, RT, 16 h, 4% for **13**, 22% for **14**.

In order to access the quaternary-methyl analogues, the indazole was protected as the *N*-Boc derivative. In the cases where the parent acrylic acid was used as starting material, this also formed the *tert*-butyl ester. Treatment of the protected indazole with cerium(IV) ammonium nitrate in acetonitrile/water formed the iminium ion, which could be reacted with methylmagnesium bromide to form the quaternary centre as a single diastereoisomer, albeit in low yield. Hydrolysis of the *N*-Boc and ester groups afforded the acrylic acids **16-18** (Scheme 7).

1
2 **Scheme 7. Oxidation / Grignard approach to the quaternary substituted core^a**
3
4



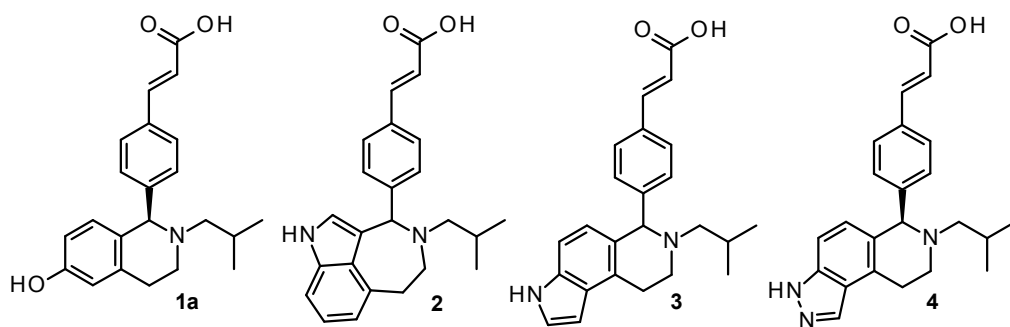
32
33
34
35
36
37
38
39
40
41
42
43
44
45
46
47
48
49
50
51
52
53
54
55
56
57
58
59
60

^aReagents and Conditions: (a) R₃=H: Boc₂O, DMAP, ^tBuOH, 80 °C, 4 h, 97% for **16a**, 36% for **17a**;
R₃=Me: Boc₂O, DMAP, DCM, RT, 1 h, 100% for **18b**; (b) cerium(IV) ammonium nitrate, MeCN, H₂O,
RT, 2 h, then MeMgBr, THF, -78 °C to 0 °C, 1 h, 12-41%; (c) R₃=^tBu: 4N HCl in dioxane, RT, 2-3 h,
88% for **16**, 94% for **17**; R₃=Me: 4N HCl in dioxane, RT, 1 h, then 2N NaOH, THF, MeOH, RT, 2 h,
51% for **18**.

Biological evaluation

Profiling of the isomeric indole **2** by-product showed only weak binding in the enzyme and no activity in the ER α degradation assay as expected. In contrast, the desired indole **3** showed good binding potency and maintained the desired degrader-antagonist profile, although it was >10 fold less potent than the THIQ **1a**. Given the weaker activity of the racemate of **3**, the individual enantiomers were not separated. In contrast however, the most active enantiomer²⁸ of indazole **4** was of similar potency and only slightly more lipophilic ($\Delta\log D_{7.4} +0.4$) relative to the THIQ phenol matched pair **1a** (**10a** in previous paper¹¹). This also showed no evidence of trapping in the microsome based GSH assay (Table 1).

Table 1. Data for phenol, indazole and indole cores.

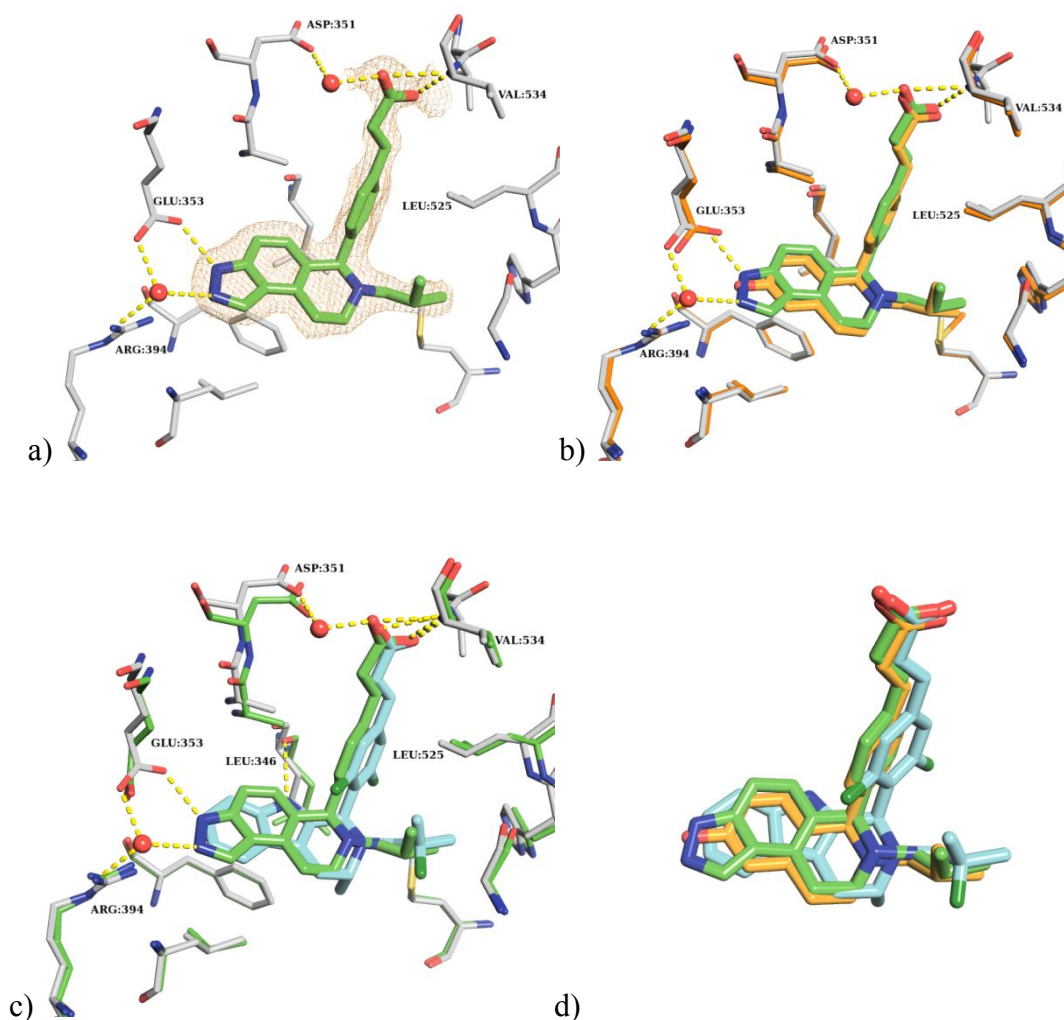


Cpd	ER bind pIC ₅₀ ^a	ER DR pIC ₅₀ ^b	LogD _{7.4} ^c	Rat/Human % Free ^d	Rat/Human hepatocyte CLint (μL/min/10 ⁶ cells) ^e	GSH trapping ratio ^f
1a	7.6	8.4	1.3	3.7/6.3	38/38	<0.04
2	4.4 ^h	<5 ^h	1.0	- /11	10/ -	-
3	6.5	7.2	1.7	6.8/3.3	20/8	-
4	7.6 ^g	8.2	1.9	3.6/7.0	10/51	<0.04

^aER binding based on $n \geq 3$ with SEM within 0.2 units, unless otherwise stated; ^bER degradation based on $n \geq 3$ with SEM within 0.2 units, unless otherwise stated; ^clogD_{7.4} determined by shake flask method; ^dDetermined from DMSO stock solution by equilibrium dialysis in 10% plasma from Alderley Park Han Wistar rats or 10% human plasma supplied by Quintiles; ^eRate of metabolism (μl/min/10⁶ cells) determined from DMSO stock solution in isolated hepatocytes diluted to 1x10⁶ cells/mL; ^fRatio of GSH trapping in human liver microsomes as a ratio to clozapine as detailed in reference 23; ^gSEM 0.50; ^hn=1.

An X-ray structure (PDBcode 6iar) of the indazole **4** complexed with an ER α ligand binding domain construct (Figure 2a) showed that the nitrogens of the tricyclic indazole interacted with a conserved water and directly with Glu-353 with distances of 3.3 and 2.8 Å respectively. The indazole scaffold showed a similar interaction network and occupied a similar binding pose in the ER α binding site (Figure 2b) with

1
2 minimal perturbation of the ligand position with respect to the THIQ scaffold.¹¹ Furthermore, overlay
3 with the structure of **1b** (Figure 2c) showed close alignment of the [5.6.6] ring system of the tricyclic
4 indazole with the [6.5.6] core of the tricyclic indole.⁸ For the tricyclic indazole core the interaction
5 network differed with additional interactions with the indazole and the salt bridge (Figure 2a). The
6 hydrogen bond between the indole of **1b** and Leu-346 was not replicated in the indazole scaffold structure
7 (Figure 2c). The different ligand binding site interaction networks observed between the different series
8 resulted in slight perturbation of the key binding motifs (Figure 2d) of the series within the ER α binding
9 domain.
10
11
12
13
14
15
16
17
18 domain.

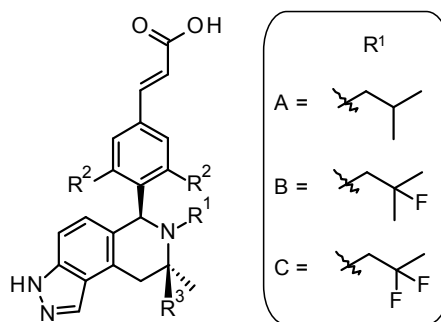


1
2 **Figure 2.** (a) X-ray crystallography of indazole **4** bound to the ER α ligand binding domain construct
3 (pdbcode 6iar); (b) overlaid with THIQ **1a** coloured orange (**10a** from ref 11; pdbcode 5fqr); (c) overlaid
4 with **1b** coloured blue (from ref 8; pdbcode 5acc); (d) superimposition of ligands **1a** and **1b** with **4**.
5
6
7
8
9

10
11 Given the high similarity of ligand binding between the three scaffolds, we applied some of the known
12 SAR from our previous work¹¹ to increase potency. The 3,3-*gem*-dimethyl substituted core (**5**) was more
13 potent than the unsubstituted core (**4**) in agreement with previous SAR. The mono substituted 3-(*R*)-
14 methyl group (**6**) increased potency further providing our first sub-nanomolar degrader-antagonist (pIC₅₀
15 9.2).²⁹ The core modification from 3-(*R*)-methyl to 3,3-*gem*-dimethyl (exemplified by **6** to **5**) had been
16 shown previously to be beneficial for lowering human hepatocyte clearance however, in this series the
17 turnover was consistently higher.³⁰ We then added fluorine atoms to the alkyl chain in the β -position to
18 the nitrogen (**7**) and in the 2,6-positions of the aryl ring (**8**) as well as making the combination of both
19 changes (**9**). Indazole **9** has the same alkyl and aryl substitution pattern as **1b**, allowing a direct
20 comparison of the scaffolds, and was a key compound for our evaluation of the indazole series.
21
22
23
24
25
26
27
28
29
30
31
32
33
34
35

36 Although the compounds were reasonably metabolically stable in rat hepatocytes, the high turnover in
37 human hepatocytes for compounds **5-7** was cause for concern. Whilst fluorination of the aryl ring (**8**, **9**)
38 ameliorated this to some degree, further improvements were sought. Notably switching the alkyl chain
39 from the 2-fluoro-isobutyl to a 2,2-difluoro-isopropyl (**10**) substituent, lowered both lipophilicity and
40 human hepatocyte clearance whilst maintaining downregulation potency. Notably, none of these
41 indazoles showed any evidence of trapping in the GSH assay, in stark contrast to the previously reported
42 phenols (Table 2).³¹
43
44
45
46
47
48
49
50
51
52
53
54

55 **Table 2. Data for methyl and fluoro substitutions of the core, alkyl chain and aryl ring.^a**
56
57
58
59
60



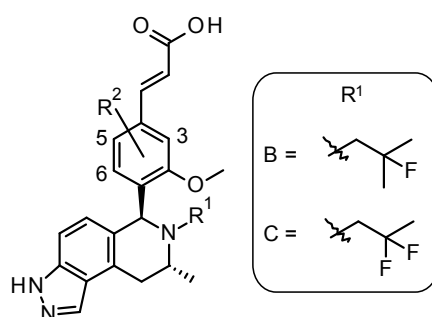
Cpd	R ¹	R ²	R ³	ER bind pIC ₅₀	ER DR pIC ₅₀	LogD _{7.4}	Rat/Human % Free	Rat/Human hepatocyte Clint (μL/min/10 ⁶ cells)	GSH trapping ratio
5	A	H	Me	7.7	8.8	2.0	6.6/3.6	6/93	<0.04
6	A	H	H	8.0	9.2	-	3.4/2.2	7/30	<0.04
7	B	H	H	8.8	9.5	2.9	1.5/0.87	8/78	-
8	A	F	H	8.9	9.1	3.0	0.52/0.48	19/22	<0.04
9	B	F	H	9.5	9.6	2.6	0.83/0.58	26/17	<0.04
10	C	F	H	9.4	9.4	2.3	1.3/1.1	18/8	<0.04

^aLegend as Table 1.

Further optimization revealed that a 2-methoxy substituent was tolerated in the aryl ring resulting in similar levels of potency and lipophilicity (compounds **11** & **12** are matched pairs of **9** & **10**). This change further lowered turnover in human hepatocytes and the compounds were clean when tested in the GSH trapping assay. Systematic exploration of the effect of fluorine

substitution on the aryl ring (**13-15**) showed that the 3-F (**13**) lost potency (20x relative to **5**), the 5-F (**14**) was equipotent and the 6-F (**15**) was the most potent compound synthesized in this series (Table 3).

Table 3. Data for alkyl chain and aryl ring variation in the 2-methoxy aryl series.

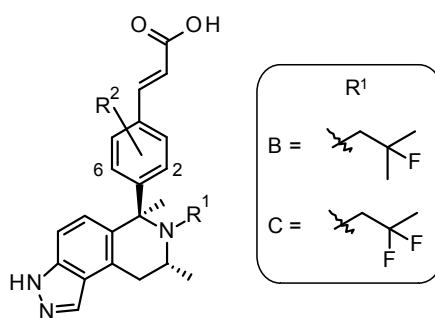


Cpd	R ¹	R ²	ER bind pIC ₅₀	ER DR pIC ₅₀	LogD _{7,4}	Rat/Human % Free	Rat/Human hepatocyte Clint (μL/min/10 ⁶ cells)	GSH trapping ratio
11	B	H	8.8	9.2	2.2	4.6/0.98	17/6	<0.04
12	C	H	9.0 ^b	9.0	2.5	2.2/0.92	18/5	<0.04
13	C	3-F	8.9	8.2	2.6	- /0.82	17/7	-
14	C	5-F	9.3	9.5	2.6	- /1.2	22/5	-
15	C	6-F	9.5	9.7	2.8	- /0.7	32/6	-

^aLegend as Table 1; ^bSEM 0.50.

We then turned our attention to the 1-methyl substitution. We had previously investigated this transformation (H→Me) in the THIQ phenol series and found it added lipophilicity and lowered potency ($\Delta\log D_{7.4} +0.9$; $\Delta pIC_{50} -0.4$ for 1-H (**10a**) to 1-Me (**11a**) in ref 11). Despite this discouraging result, we made the corresponding 1-methyl matched pairs in the indazoles and found with the 2,6-difluoro aryl ring a more modest rise in lipophilicity and small drop in potency (**16** & **9** $\Delta\log D_{7.4} +0.3$; $\Delta pIC_{50} -0.3$ and **17** & **10** $\Delta\log D_{7.4} +0.7$; $\Delta pIC_{50} -0.3$). By contrast, with the 2-methoxy aryl, addition of the 1-Me *decreased* lipophilicity and showed a bigger drop in potency (**18** & **11** $\Delta\log D_{7.4} -0.3$; $\Delta pIC_{50} -0.6$) as shown in Table 4. To probe this surprising and divergent SAR, we considered the effect of the aryl substituent in terms of conformation using a combination of computational and NMR techniques.

Table 4. Data for 1-methyl substituted indazoles.^a



Cpd	R ¹	R ²	ER bind	ER DR	LogD _{7.4}	Rat/Human % Free	Rat/Human hepatocyte Clint ($\mu\text{L}/\text{min}/10^6$ cells)	GSH trapping ratio
16	B	2,6-F,F	9.4	9.2	2.9	0.23/0.33	12/10	<0.04
17	C	2,6-F,F	9.5	9.1	3.0	0.76/0.27	20/6	-

1									
2	18	B	2-OMe	8.4	8.6	1.9	-17.7	10/4	-
3									
4									

5 ^aLegend as Table 1

6
7
8
9
10
11 To investigate the influence of the *ortho*-substituent on the mobility of the aryl ring further we
12
13 carried out an NMR conformational analysis study on compounds **10**, **12**, **15** and **18** with the
14
15 results shown in Figure 3. Di-fluoro aryl compound **10** showed one single ¹H and ¹⁹F resonance
16
17 respectively for the 2 hydrogen and 2 fluorine atoms in the aryl ring, indicating that both *ortho*-F
18
19 and *meta*-H were exposed to the same chemical environment in the NMR time-scale (*i.e.* the
20
21 aryl group is freely rotating). ¹H and ¹⁹F n.O.e. based experiments established that the *N*-alkyl
22
23 chain adopted a preferred conformation with the hydrogens in the α -position and the fluorine
24
25 atoms in the β -position pointed away from the aryl ring, in close agreement with the X-ray
26
27 structure of **1b** (pdbcode 5acc). Incorporation of an *ortho*-OMe group in the aryl ring (**12**) had a
28
29 very significant effect on the rotational flexibility of the ring as observed by NMR. In this case,
30
31 the aryl ring showed a restricted rotation, with the n.O.e.'s between the *ortho*-OMe/H and the
32
33 rest of the molecule consistent with the methoxy group pointing away from the core ring. The
34
35 restricted rotation of the aryl ring did not affect the conformation of the *N*-alkyl chain, which was
36
37 identical to that observed for compound **10**. Further substitution of the *ortho*-H with a F (**15**) did
38
39 not alter the rigidity and orientation of the aryl ring or the *N*-alkyl chain compared with **12**, with
40
41
42
43
44
45
46
47
48
49
50
51
52
53
54
55
56
57
58
59
60

1
2 the OMe group still favouring the alignment away from the ring. The incorporation of a methyl
3
4
5
6 group in the benzylic position (**18**) however, inverts the orientation of the aryl ring, with the OMe
7
8
9 group now positioned towards and on top of the core ring to avoid clashing with the Me group.
10
11
12 This switch in conformational locking occurs presumably due to steric reasons and we believe is
13
14
15 responsible for the divergent behavior observed in terms of both the potency and lipophilicity
16
17
18 with pairs **16** & **9** and **18** & **11**. This is an example of the importance of considering molecular
19
20
21 conformation when interpreting data and highlights the utility of computational and NMR based methods
22
23
24 to provide an insight into the rigidity and flexibility of ligands in solution.
25
26
27
28
29
30
31
32
33
34
35
36
37
38
39
40
41
42
43
44
45
46
47
48
49
50
51
52
53
54
55
56
57
58
59
60

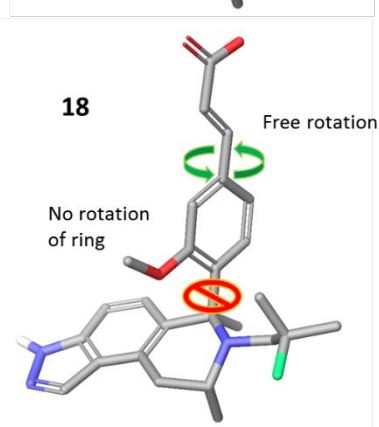
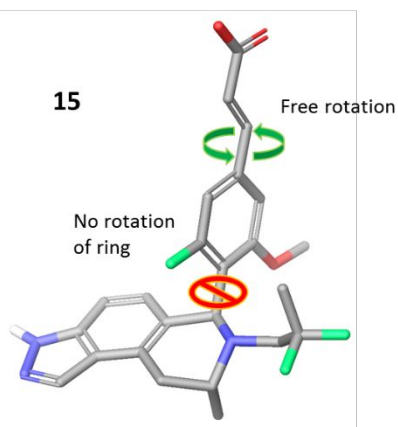
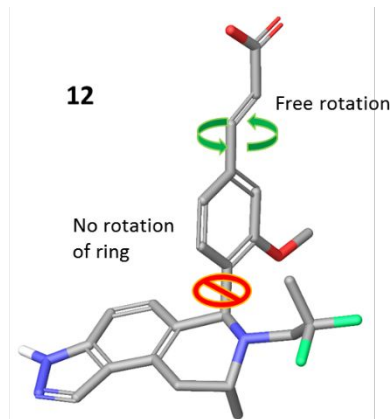
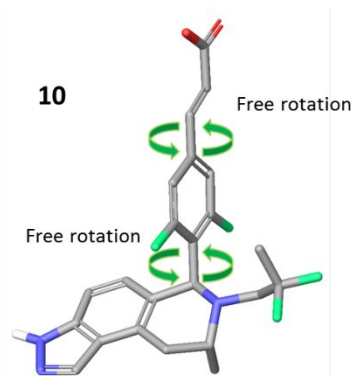


Figure 3. Experimentally derived NMR based conformations of **10**, **12**, **15** and **18** showing free rotation of the 2,6-F,F aryl ring of **10** in contrast to the locked conformations of **12** & **15** (which orient the 2-OMe substituent away from the core) and **18** (which contrastingly orients the 2-OMe substituent towards the core).

Physicochemical & DMPK profiling

In terms of physicochemical properties, the indazole acids were found to have high permeability with minimal efflux (based on Caco-2 and MDCK assays) and good solubility in aqueous media with representative examples shown in Table 5. The plasma protein binding data was measured in mouse and dog, with similar values being obtained to those in rat and human respectively. Screening against a panel of five cytochrome P450 enzymes in a high throughput human liver microsome assay showed no activity (IC_{50} values $> 30 \mu M$) against 3 isoforms (CYP1A2, CYP2C19, CYP2D6) however modest inhibition of CYP2C9 was observed in both cases. Indazole **9** showed weak activity (IC_{50} $13 \mu M$) against CYP3A4 however this could be removed by subtle changes to the alkyl chain (*e.g.* **10** $IC_{50} > 30 \mu M$). No discernable activity ($IC_{50} > 30 \mu M$) against the hERG ion channel was observed for any of the examples tested from this series.

Table 5. Physicochemical & *in vitro* DMPK data for selected indazoles.

Cpd	Caco2	MDCK P_{app}	Sol (μM) ^b	Mu/Rat/Dog %	CYP 2C9	CYP 3A4	hERG
-----	-------	----------------	------------------------------	--------------	---------	---------	------

	P_{app}	(efflux ratio) ^a	Free	(μM) ^c	(μM) ^c	(μM) ^d	
9	6.9 (1.4)	11 (0.6)	>1000	0.95/0.83/0.32	2.5	13	>100
10	5.8 (2.6)	10 (1.3)	760	2.1/1.3/0.62	6.6	>30	>100
12	6.2 (2.2)	8.4 (1.7)	810	1.2/2.2/0.87	-	-	-

^aCompounds were incubated at 10 μM in cultured Caco-2 or MDCK cells. Permeability was measured in both the apical to basolateral (A to B) and basolateral to apical (B to A) directions. Efflux ratio is expressed as (B to A) / (A to B); ^bSolubility of compounds in aqueous phosphate buffer at pH 7.4 after 24 h at 25 °C; ^cInhibition of cytochrome P450 enzymes IC_{50} . ^dInhibition of the hERG tail current was measured using a plate-based planar patch clamp system (IonWorks™).

We also investigated the chemical stability of these compounds, initially using an NMR based approach. Compounds were dissolved in deuterated buffers (pH 4 and 7.4) and ¹H NMR spectra were recorded at several time points over a period of 8 d. Unchanged spectra after that time indicate that the compound was stable under those conditions but modification of the NMR spectra (*e.g.* reduction of parent signals, appearance of new resonances) was indicative that a

1
2 degradative process was taking place. Whilst **9** was completely stable at pH 7.4, some
3
4
5
6 instability was noted at pH 4 (58% of compound remaining after 8 d in buffer). By contrast,
7
8
9 compound **12** showed no degradation after 8 d at either pH 4 or 7.4. Subsequent profiling
10
11
12 showed that **12** showed no instability under forcing conditions (at pH 1, 4, or 10). This stability
13
14
15
16 was in notable contrast to that reported by Novartis on their phenolic THIQ scaffold where
17
18
19 racemization was observed and proposed to occur *via* a quinoline intermediate.¹³ We believe
20
21
22
23 that the combination of the less electron rich indazole together with the transannular methyl
24
25
26 group, which favours the thermodynamically more stable 1,3-*trans* arrangement, is responsible
27
28
29
30 for the enhanced stability of this scaffold relative to *geminal*-disubstituted phenolic THIQs.
31
32
33
34
35
36

37 The *in vitro* hepatocyte and *in vivo* pharmacokinetic (non-compartmental) properties of **9**, **10**
38
39
40 and **12** were investigated in rat and dog and their values are reported in Table 6. *In vitro*
41
42
43 clearance was moderate in both rat (18-26 $\mu\text{L}/\text{min}/10^6$ cells) and dog (7-17 $\mu\text{L}/\text{min}/10^6$ cells)
44
45
46
47 with **10** and **12**, which contain the 2-OMe aryl ring, showing lower turnover than **9** which
48
49
50
51 contains the 2,6-F,F aryl. *In vivo* clearance in rats was low to moderate and ranged from 33-
52
53
54 46% and 7-15% of hepatic blood flow in rat and dog respectively. Scaling of *in vitro* clearance
55
56
57
58 with free fraction and blood/plasma ratio yielded an *in vitro* / *in vivo* correlation within 2-fold
59
60

(data not shown). Volume of distribution was low to moderate in both rat and dog and is consistent with the highly protein bound and acidic properties of these compounds. Bioavailability was generally good (16-51%) for **9**, **10** and **12** and is reflective of the high *in vitro* permeability combined with low/moderate clearance. These properties were deemed suitable to pursue *in vivo* pharmacodynamics studies.

Table 6. Summary of Pharmacokinetic Parameters after IV and PO dosing in rat and dog. ^a

Cpd	Species	Clint ($\mu\text{L}/\text{min}/10^6$ cells)	Dose ^a IV/PO (mg/kg)	CL (mL/min/kg)	Vd _{ss} (L/kg)	t _{1/2} (hr)	%F	PO AUC ($\mu\text{M}\cdot\text{hr}$)
9	Rat	26	0.5/1	23	1.6	1.2	31	0.83
10	Rat	18	0.5/1	26	1.6	3.7	16	0.57
12	Rat	18	0.5/1	32	1.0	1.3	51	0.21
9	Dog	17	0.5/1	5.9	0.58	6.1	45	3.2
10	Dog	7.1	0.5/1	5.4	0.63	4.8	36	3.0
12	Dog	9.6	0.5/1	2.8	0.36	6.8	45	6.6

^aCompounds were dosed in rat and dog intravenously at 0.5 and orally at 1 mg/kg. The formulation by both routes was 5% DMSO:95% hydroxypropyl β -cyclodextrin (30% w/v) at a volume of 1 mL/kg and 4 mL/kg, IV and PO respectively.

Pharmacological profiling of compound **9**

The pharmacology of compound **9** was profiled as previously described for **1b**.³² As shown in Figure 4, the curves from the ER α downregulation assay (Figure 4a), tamoxifen competition assay (Figure 4b) and ER α antagonism assay (Figure 4c) were consistent with the desired degrader-antagonist profile with no evidence of ER agonism as measured in the progesterone receptor (PR) assay, a downstream marker for ER α transcriptional activation (Figure 4a).

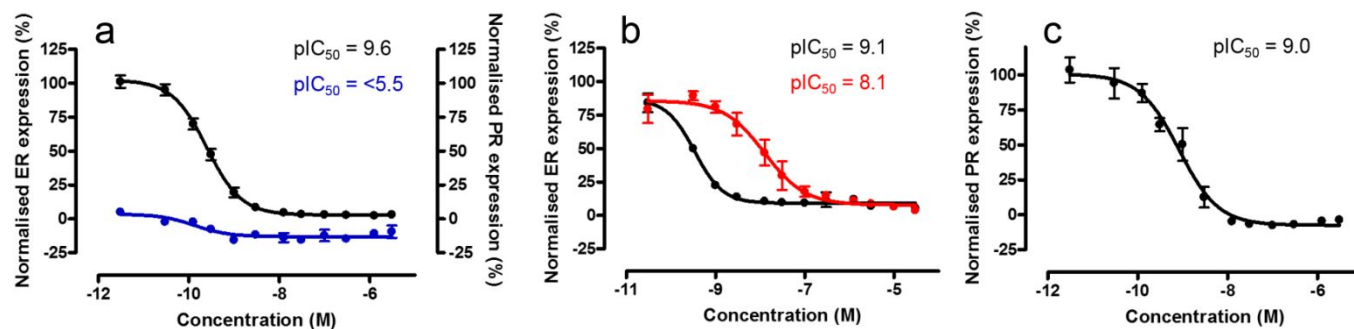


Figure 4. (a) ER α (black) and PR (blue) protein expression in the MCF-7 cell line after treatment with compound **9** showing a concentration dependent decrease in ER α expression and no increase in PR expression consistent with no ER agonism; (b) ER α protein expression curve (black) and decrease in potency in the presence of 0.25 μ M tamoxifen (red) due to competition at the ER α ligand binding site; (c) Concentration-dependent decrease by **9** in estradiol-driven PR response as a measure of ER antagonism.

The ability of **9** to downregulate ER α was also investigated by Western blot. MCF-7 cells were incubated with either **9** or fulvestrant for 24 h at a range of concentrations and total protein was extracted and immunoblotting performed to detect effects on ER α protein expression. As shown in Figure 5, both **9** and fulvestrant proved to be potent degraders of ER α in MCF-7 cells.

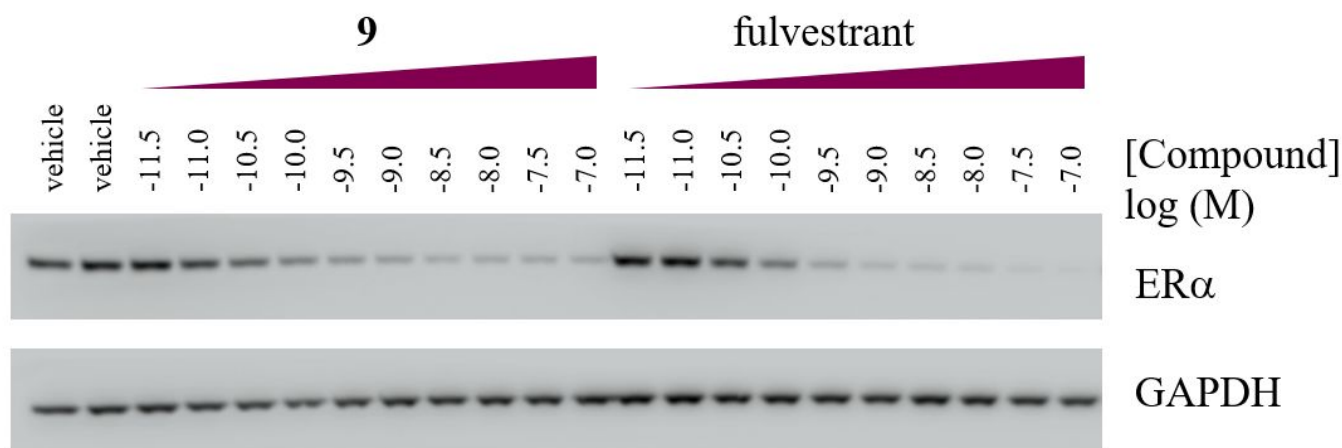


Figure 5. Concentration-dependent degradation of ER α by **9** and fulvestrant by Western blot analysis.

Compound **9** was also investigated in terms of its antiproliferative capability. As shown in Figure 6, a concentration-dependent decrease in estradiol-driven cell growth of the MCF-7 cell line was observed with **9** (Figure 6a) giving a similar potency (pIC_{50} 8.2) to that observed with fulvestrant (pIC_{50} 8.3; Figure 6b).

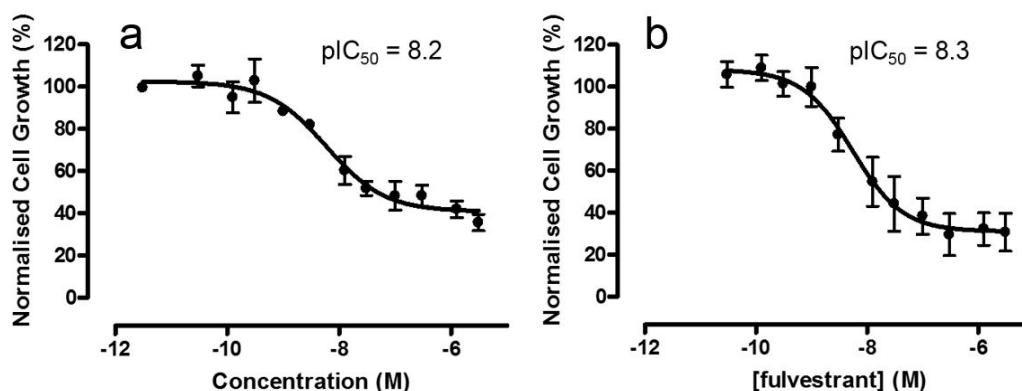
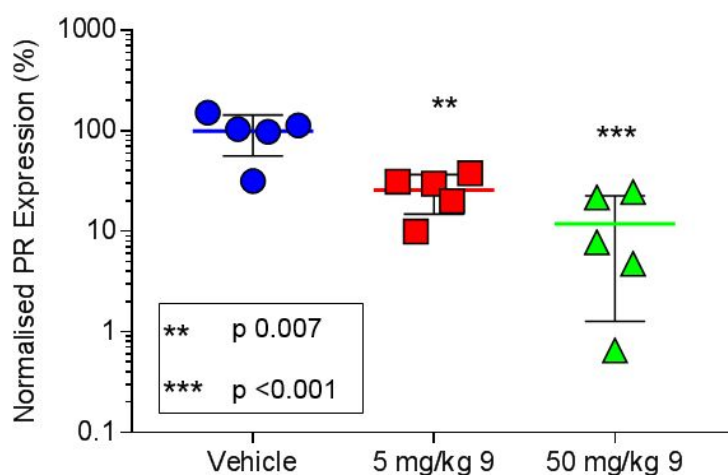


Figure 6. Concentration-dependent decrease in estradiol-driven cell growth of the MCF-7 cell line with **9** (A) and fulvestrant (B).

1
2
3
4
5
6 *In vivo* profiling was carried out to investigate the ability of **9** to effect reduction of PR levels
7
8
9 (Figure 7) and tumour growth (Figure 8) in an MCF-7 xenograft model. MCF-7 xenografts, grown in
10
11
12 male SCID mice, were orally dosed once daily with either PEG/captisol (vehicle) or **9** at the doses shown.
13
14
15
16 After 3 d of dosing, tumours were collected 24 h after the last dose and 5 mg/kg was found to
17
18
19 reduce the normalized PR levels by 74% ($p = 0.007$) and at 50 mg/kg by 93% ($p < 0.001$).
20
21
22
23
24
25



26
27
28
29
30
31
32
33
34
35
36
37
38
39
40
41
42 **Figure 7.** Dose-dependent decrease in PR levels, measured by Western blotting, following oral dosing of
43
44
45 **9** to mice once daily in an MCF7 mouse tumour xenograft model. MCF-7 xenografts were dosed
46
47
48 for 3 d with doses shown and tumours collected at 24 h after the last dose.
49
50

51
52
53
54
55 Compound **9** was then evaluated for effect on tumour growth in the same MCF-7 xenograft model
56
57
58 (Figure 8). At doses of 20 mg/kg administered orally once daily, compound **9** was able to effect
59
60 significant tumour growth inhibition (80%) at 20 d in this model and was well tolerated.

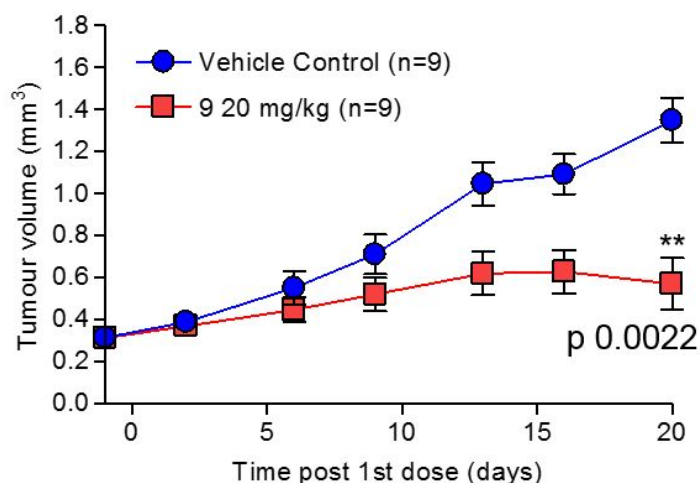


Figure 8. Antitumour activity of **9** administered orally once daily at 20 mg/kg in MCF-7 xenografts.

CONCLUSIONS

In conclusion, we have demonstrated that the phenol of our previously reported tetrahydroisoquinoline scaffold could be successfully replaced by an indazole group and that this led to removal of a reactive metabolite signal in a glutathione *in vitro* trapping assay. Optimization of the alkyl sidechain and pendant aryl group gave compounds that showed low turnover in human hepatocytes and good chemical stability. Compound **9** was profiled as a representative of the series in terms of pharmacology and demonstrated the desired ER α degrader-antagonist profile and demonstrated activity in a xenograft model.

EXPERIMENTAL SECTION

General Procedures: All solvents and chemicals used were reagent grade. Anhydrous solvents THF, DCM, and DMF were purchased from Aldrich. Solutions were dried over anhydrous magnesium sulfate or sodium sulfate, and solvent was removed by rotary evaporation under reduced pressure. Microwave reactions were run in a Biotage 'Initiator Robot 60' (100-120/220-240 V, 50-60 Hz, 100 VA). Flash column chromatography was carried out using prepacked silica cartridges (from 4 g up to 330 g) from Grace, Redisep or Silicycle and eluted using an Isco Companion system. The purity of compounds submitted for screening was >95% as determined by UV analysis of liquid chromatography-mass spectroscopy (LCMS) chromatograms at 254 nm and substantiated using the TAC (Total Absorption Chromatogram). Further support for the purity statement was provided using the MS TIC (Total Ion Current) trace in ESI +ve and -ve ion modes, HRMS and NMR analysis. NMR spectra were recorded on a Varian INOVA (600 MHz), Varian Gemini 2000 (300 MHz), Bruker Avance 700 (700 MHz), Bruker Avance 500 (500 MHz) or Bruker Avance DPX400 (400 MHz) and were determined in CDCl₃, DMSO-*d*₆, or MeOH-*d*₄. Chemical shifts are reported in ppm relative to TMS (0.00 ppm) or solvent peaks as the internal reference. Splitting patterns are indicated as follows: s, singlet; d, doublet; t, triplet; m, multiplet; br, broad peak. Analytical LCMS was carried out using a suitable system, such as a Waters 2790/95 LC system with a 2996 PDA and a 2000 amu ZQ single quadrupole mass spectrometer, or a UPLC system utilising a Waters Aquity Binary pump with sample manager, Aquity PDA and SQD Mass spectrometer. Accurate mass and MSMS fragmentation data were obtained using a Thermo Scientific hybrid LTQ-FT Mass Spectrometer with an Agilent 1100 Quaternary pump with PDA and Autosampler; 5 μL of sample dissolved in 50:50 acetonitrile:water 0.1% formic acid was injected onto a Thermo Scientific Hypersil Gold 50 x 2.1 mm 5 μm particle LC Column and eluted with a gradient of 5 to 100% B over 17 min with 3 min re-equilibration time at 5% B. The flow rate was 0.5 mL/min with A being 0.1% formic acid in water and B 0.1% formic acid in acetonitrile. The MS and MSMS spectra were obtained in ESI +ve mode in both the ion trap and Ion Cyclotron Resonance (ICR) cell using helium as the collision gas at a normalised collision energy of 35 eV. The ICR cell was run at resolution settings of 25000 in MS mode and 12500 in MSMS mode.

1 All IC₅₀ data are quoted as geometric mean values, and statistical analysis is available in the Supporting
2 Information.
3

4
5
6 All experimental activities involving animals were carried out in accordance with AstraZeneca animal
7 welfare protocols which are consistent with The American Chemical Society Publications rules and
8 ethical guidelines.
9
10

11
12
13 **(E)-3-(4-(4-isobutyl-3,4,5,6-tetrahydro-1H-azepino[3,4,5-cd]indol-3-yl)phenyl)acrylic acid (2).** 7.5M

14 Sodium hydroxide solution (0.062 mL, 0.46 mmol) was added to a solution of (E)-methyl 3-(4-(4-
15 isobutyl-3,4,5,6-tetrahydro-1H-azepino[3,4,5-cd]indol-3-yl)phenyl)acrylate (0.018 g, 0.05 mmol) in
16 MeOH (1 mL) and THF (1.0 mL). The mixture was stirred at 20 °C for 24 hours. The mixture was
17 concentrated to a volume such that the organic solvent had been removed then diluted with water (20 mL)
18 and the aqueous layer taken to pH 7 with 1M citric acid. The mixture was extracted into ethyl acetate (3 x
19 100 mL) and the combined organics were washed with brine (100 mL), dried over MgSO₄, filtered and
20 evaporated to give crude product which was purified by flash silica chromatography, elution gradient 0 to
21 10% MeOH in DCM. Pure fractions were evaporated to dryness to afford (E)-3-(4-(4-isobutyl-3,4,5,6-
22 tetrahydro-1H-azepino[3,4,5-cd]indol-3-yl)phenyl)acrylic acid (0.015 g, 86%) as a white solid. ¹H NMR
23 (500 MHz, DMSO, 27 °C) 0.89 (d, *J* = 6.5 Hz, 6H), 1.86 (m, 1H), 2.35 (m, 1H), 2.47 (m, 1H), 2.82 (m,
24 1H), 2.88 (m, 1H), 3.09 (m, 1H), 3.29 (m, 1H), 5.22 (s, 1H), 6.41 (d, *J* = 16.0 Hz, 1H), 6.73 (d, *J* = 7.1
25 Hz, 1H), 6.90 (d, *J* = 2.4 Hz, 1H), 6.97 (dd, *J* = 8.1, 7.1 Hz, 1H), 7.11 (d, *J* = 8.2 Hz, 2H), 7.18 (d, *J* = 8.0
26 Hz, 1H), 7.40 (d, *J* = 16.0 Hz, 1H), 7.49 (d, *J* = 8.4 Hz, 2H), 10.97 (d, *J* = 2.5 Hz, 1H); ¹³C NMR (125
27 MHz, DMSO, 27 °C) 20.7, 20.7, 25.9, 33.0, 47.8, 60.3, 65.0, 108.7, 115.6, 118.1, 120.7, 120.9, 123.7,
28 125.6, 127.4 (2C), 128.8 (2C), 133.0, 133.7, 136.6, 141.6, 147.7, 168.4; *m/z*: ES+ [M+H]⁺ 375; HRMS
29 (ESI) for C₂₄H₂₆N₂O₂ (MH⁺); calcd, 375.2067; found, 375.2068.
30
31

32
33
34 **(E)-3-(4-(7-isobutyl-6,7,8,9-tetrahydro-3H-pyrrolo[3,2-f]isoquinolin-6-yl)phenyl)acrylic acid (3).**

35
36
37 7.5M Sodium hydroxide solution (0.240 mL, 1.80 mmol) was added to a solution of (E)-methyl 3-(4-(7-
38 isobutyl-6,7,8,9-tetrahydro-3H-pyrrolo[3,2-f]isoquinolin-6-yl)phenyl)acrylate (0.07 g, 0.18 mmol) in
39 MeOH (2 mL) and THF (2 mL). The mixture was stirred at 20 °C for 24 hours. The mixture was
40
41
42
43
44
45
46
47
48
49
50
51
52
53
54
55
56
57
58
59
60

1 concentrated to a volume such that the organic solvent had been removed then diluted with water (20 mL)
2
3 and the aqueous layer was taken to pH 7 with 1M citric acid. The mixture was extracted into ethyl acetate
4
5 (3 x 100 mL) and the combined organics washed with brine (100 mL), dried over MgSO₄, filtered and
6
7 evaporated to give a solid. The crude product was purified by flash silica chromatography, elution
8
9 gradient 0 to 10% MeOH in DCM. Pure fractions were evaporated to dryness to afford (*E*)-3-(4-(7-
10
11 isobutyl-6,7,8,9-tetrahydro-3H-pyrrolo[3,2-*f*]isoquinolin-6-yl)phenyl)acrylic acid (0.041 g, 61%) as a
12
13 white solid. ¹H NMR (500 MHz, DMSO, 27 °C) 0.72 (d, *J* = 6.5 Hz, 3H), 0.77 (d, *J* = 6.5 Hz, 3H), 1.83
14
15 (ddt, *J* = 15.6, 12.8, 6.6 Hz, 1H), 2.08 (dd, *J* = 12.3, 9.2 Hz, 1H), 2.17 (dd, *J* = 12.3, 5.3 Hz, 1H), 2.5 –
16
17 2.55 (m, 1H), 2.92 – 3.09 (m, 2H), 3.17 (dt, *J* = 10.9, 5.0 Hz, 1H), 4.59 (s, 1H), 6.38 (d, *J* = 8.5 Hz, 1H),
18
19 6.41 (t, *J* = 2.4 Hz, 1H), 6.45 (d, *J* = 16.0 Hz, 1H), 7.03 (d, *J* = 8.4 Hz, 1H), 7.25 (d, *J* = 7.9 Hz, 2H), 7.27
20
21 (t, *J* = 2.8 Hz, 1H), 7.52 (d, *J* = 16.0 Hz, 1H), 7.56 (d, *J* = 8.0 Hz, 2H), 10.97 (d, *J* = 2.4 Hz, 1H), 12.39 (s,
22
23 1H); ¹³C NMR (125 MHz, DMSO, 27 °C) 20.5, 20.9, 25.4, 25.7, 46.4, 62.4, 67.9, 99.2, 109.2, 119.1,
24
25 121.9, 124.7, 125.6, 126.3, 127.3, 127.7 (2C), 129.9 (2C), 132.7, 133.5, 143.4, 147.7, 167.7; *m/z*: ES+
26
27 [M+H]⁺ 375; HRMS (ESI) for C₂₄H₂₆N₂O₂ (MH⁺); calcd, 375.2065; found, 375.2065.

28
29
30
31
32
33
34 **(*E*)-3-(4-(7-isobutyl-6,7,8,9-tetrahydro-3H-pyrazolo[4,3-*f*]isoquinolin-6-yl)phenyl)acrylic acid (4).** A
35
36 solution of (*E*)-*tert*-butyl 3-(4-(7-isobutyl-6,7,8,9-tetrahydro-3H-pyrazolo[4,3-*f*]isoquinolin-6-
37
38 yl)phenyl)acrylate (600 mg, 1.39 mmol) in dichloromethane (4 mL) was treated with trifluoroacetic acid
39
40 (2 mL) and the reaction mixture was stirred at room temperature for 45 min. The solvent was removed
41
42 under reduced pressure and the residue was treated with excess aqueous sodium bicarbonate and the
43
44 resultant precipitate was dissolved in a mixture of water and 2M aqueous sodium hydroxide solution. The
45
46 pH was adjusted to ~6 by addition of acetic acid and the mixture was extracted with 2-methyl
47
48 tetrahydrofuran (x2), the combined organics were dried, filtered and evaporated under reduced pressure.
49
50 The crude product was purified by flash silica chromatography eluted with a gradient of 0-10% methanol
51
52 in dichloromethane to yield 480 mg of racemic product which was purified by preparative HPLC
53
54 (Chiralpak IA column, 20 μm silica, 100 mm diameter, 250 mm length), Heptane:EtOH 80:20 at 350 ml /
55
56 min. Fractions containing the desired compounds were combined and evaporated to dryness to afford the
57
58
59
60

1
2 desired enantiomer (225 mg, 38%) as a solid. ¹H NMR (400 MHz, DMSO, 27 °C) 0.72 (3H, d), 0.77 (3H,
3 d), 1.77 - 1.88 (1H, m), 2.03 - 2.13 (1H, m), 2.19 (1H, dd), 2.52 - 2.59 (1H, m), 3.06 - 3.21 (3H, m), 4.62
4 d), 1.77 - 1.88 (1H, m), 2.03 - 2.13 (1H, m), 2.19 (1H, dd), 2.52 - 2.59 (1H, m), 3.06 - 3.21 (3H, m), 4.62
5 (1H, s), 6.46 (1H, d), 6.63 (1H, d), 7.17 (1H, d), 7.26 (2H, d), 7.54 (1H, d), 7.58 (2H, d), 8.06 (1H, s),
6
7 12.93 (1H, s); m/z (ES+) (M+H)+ = 376.

10
11 **(E)-3-(4-(7-isobutyl-8,8-dimethyl-6,7,8,9-tetrahydro-3H-pyrazolo[4,3-f]isoquinolin-6-**
12
13 **yl)phenyl)acrylic acid (5).** (*E*)-*tert*-butyl 3-(4-(7-isobutyl-8,8-dimethyl-2-(tetrahydro-2H-pyran-2-yl)-
14 6,7,8,9-tetrahydro-2H-pyrazolo[4,3-f]isoquinolin-6-yl)phenyl)acrylate (175 mg, 0.32 mmol) was stirred
15 in DCM (4 mL) and TFA (2.0 mL) at room temperature for 2 hours. The reaction mixture was purified by
16 ion exchange chromatography, using an SCX column. The desired product was eluted from the column
17 using 7M NH₃/MeOH and evaporated to dryness to afford crude product which was purified by flash
18 silica chromatography, elution gradient 0 to 10% MeOH in DCM. Pure fractions were evaporated to
19 dryness to afford racemic product which was purified by preparative HPLC (Chiralpak AD column,
20 20µm silica, 50 mm diameter, 250 mm length), Heptane/EtOH-MeOH/AcOH 90/10/0.2. Fractions
21 containing the desired compounds were evaporated (and re-purified by flash silica chromatography,
22 elution gradient 0 to 10% MeOH in DCM) to give (*E*)-3-(4-(7-isobutyl-8,8-dimethyl-6,7,8,9-tetrahydro-
23 3H-pyrazolo[4,3-f]isoquinolin-6-yl)phenyl)acrylic acid (46.0 mg, 35%) as a pale yellow solid. ¹H NMR
24 (500 MHz, DMSO, 27 °C) 0.40 (d, *J* = 6.6 Hz, 3H), 0.63 (d, *J* = 6.6 Hz, 3H), 0.90 (m, 1H) 0.91 (s, 3H),
25 1.32 (s, 3H), 2.18 (dd, *J* = 14.2, 5.7 Hz, 1H), 2.64 (dd, *J* = 14.2, 8.9 Hz, 1H), 2.94 (d, *J* = 15.9 Hz, 1H),
26 3.16 (d, *J* = 15.9 Hz, 1H), 4.66 (m, 1H), 6.44 (d, *J* = 16.0 Hz, 1H), 6.64 (d, *J* = 8.7 Hz, 1H), 7.13 (d, *J* =
27 8.7 Hz, 1H), 7.34 (m, 2H), 7.51 (d, *J* = 16.1 Hz, 1H), 7.53 (d, *J* = 8.2 Hz, 2H), 8.05 (d, *J* = 1.0 Hz, 1H),
28 12.84 (s, 2H); ¹³C NMR (126 MHz, DMSO, 27 °C) 17.4, 20.50, 20.52, 27.8, 30.6, 41.4, 53.3, 58.8, 68.6,
29 107.6, 118.8, 122.1, 125.2, 126.3, 127.8 (2C), 129.6 (2C), 129.8, 131.7, 132.7, 138.3, 143.5, 150.1, 167.7;
30 *m/z*: ES+ [M+H]⁺ 405; HRMS (ESI) for C₂₅H₂₉N₃O₂ (MH⁺); calcd, 404.2333; found, 404.2337.

31
32
33
34
35
36
37
38
39
40
41
42
43
44
45
46
47
48
49
50
51
52
53
54
55 **(E)-3-(4-((6*R*,8*R*)-7-isobutyl-8-methyl-6,7,8,9-tetrahydro-3H-pyrazolo[4,3-f]isoquinolin-6-**
56
57 **yl)phenyl)acrylic acid (6).** A solution of (*E*)-*tert*-butyl 3-(4-((6*R*,8*R*)-7-isobutyl-8-methyl-6,7,8,9-
58 tetrahydro-3H-pyrazolo[4,3-f]isoquinolin-6-yl)phenyl)acrylate (150 mg, 0.34 mmol) in dichloromethane
59

(4 mL) was treated with trifluoroacetic acid (2 mL) and the reaction mixture was allowed to stand at room temperature for 45 minutes. The solvent was removed under reduced pressure and the residue treated with excess aqueous sodium bicarbonate and the resultant precipitate was dissolved in a mixture of water and 2M aqueous sodium hydroxide solution. The pH was adjusted to ~6 by addition of acetic acid and the mixture was extracted with 2-methyl tetrahydrofuran (x2) then the combined organics were dried, filtered and evaporated under reduced pressure. The crude product was purified by flash silica chromatography eluted with a gradient of 0-10% methanol in dichloromethane to yield (*E*)-3-(4-(((6*R*,8*R*)-7-isobutyl-8-methyl-6,7,8,9-tetrahydro-3H-pyrazolo[4,3-*f*]isoquinolin-6-yl)phenyl)acrylic acid (25.0 mg, 19%) as a solid. ¹H NMR (400 MHz, DMSO, 27 °C) 0.74 (3H, d), 0.88 (3H, d), 0.98 (3H, d), 1.72 - 1.84 (1H, m), 2.03 (1H, dd), 2.28 - 2.35 (1H, m), 2.84 (1H, dd), 3.10 (2H, dd), 4.70 (1H, s), 6.45 (1H, d), 6.79 (1H, d), 7.23 (3H, d), 7.49 - 7.59 (3H, m), 8.06 (1H, s), 12.96 (1H, s); *m/z*: ES+ [M+H]⁺ 390.

(*E*)-3-(4-(((6*R*,8*R*)-7-(2-fluoro-2-methylpropyl)-8-methyl-6,7,8,9-tetrahydro-3H-pyrazolo[4,3-*f*]isoquinolin-6-yl)phenyl)acrylic acid (7). 2M sodium hydroxide (1.0 mL, 2.0 mmol) was added to a solution of (*E*)-methyl 3-(4-(((6*R*,8*R*)-3-acetyl-7-(2-fluoro-2-methylpropyl)-8-methyl-6,7,8,9-tetrahydro-3H-pyrazolo[4,3-*f*]isoquinolin-6-yl)phenyl)acrylate (95 mg, 0.20 mmol) in THF (0.50 mL) / methanol (0.50 mL). The reaction was stirred at room temperature for 1.5 hours. EtOAc and water were added and the pH of the aqueous layer was adjusted to ~6 by addition of 2N HCl. The layers were separated and the aqueous layer was extracted with EtOAc. The combined organics were dried and concentrated and the crude product was purified by flash silica chromatography, elution gradient 50 to 100% EtOAc in heptane. Pure fractions were evaporated to dryness to afford (*E*)-3-(4-(((6*R*,8*R*)-7-(2-fluoro-2-methylpropyl)-8-methyl-6,7,8,9-tetrahydro-3H-pyrazolo[4,3-*f*]isoquinolin-6-yl)phenyl)acrylic acid (69.0 mg, 83%) as a white solid. ¹H NMR (500 MHz, CDCl₃, 27 °C) 1.01 (d, *J* = 6.7 Hz, 3H), 1.26 (d, *J* = 21.5 Hz, 3H), 1.38 (d, *J* = 21.7 Hz, 3H), 2.37 - 2.46 (m, 1H), 2.76 (dd, *J* = 15.8, 6.0 Hz, 1H), 2.78 - 2.82 (m, 1H), 2.91 - 2.99 (m, 1H), 3.24 (ddd, *J* = 9.6, 6.8, 4.5 Hz, 1H), 5.04 (s, 1H), 6.45 (d, *J* = 16.0 Hz, 1H), 6.86 (d, *J* = 8.6 Hz, 1H), 7.21 (d, *J* = 8.2 Hz, 2H), 7.29 (dd, *J* = 8.5, 1.0 Hz, 1H), 7.52 (d, *J* = 16.0 Hz, 1H), 7.54 - 7.6 (m, 2H), 8.07 (d, *J* = 1.0 Hz, 1H), 12.40, (s, 1H), 13.00 (s, 1H); ¹³C NMR (125 MHz,

1
2 DMSO, 27 °C) 17.1, 24.8 (d, $J = 24.9$ Hz), 25.2 (d, $J = 23.8$ Hz), 29.0, 46.2, 54.1 (d, $J = 19.9$ Hz), 65.9,
3
4 97.6 (d, $J = 165.9$ Hz), 107.8, 118.9, 122.6, 125.5, 127.6, 127.8 (2C), 127.9, 129.5 (2C), 131.7, 132.7,
5
6 138.7, 143.5, 147.3, 167.6; ^{19}F NMR (376 MHz, DMSO, 27 °C) -137.9; m/z (ES+), $[\text{M}+\text{H}]^+ = 408$;
7
8 HRMS (ESI) for $\text{C}_{24}\text{H}_{26}\text{FN}_3\text{O}_2$ (MH^+); calcd, 408.2082; found, 408.2085.

9
10 **(*E*)-3-(3,5-difluoro-4-((6*S*,8*R*)-7-isobutyl-8-methyl-6,7,8,9-tetrahydro-3H-pyrazolo[4,3-*f*]isoquinolin-**
11
12 **6-yl)phenyl)acrylic acid (8).** 7.5M sodium hydroxide solution (3.13 mL, 23.47 mmol) was added to a

13
14 solution of (*E*)-methyl 3-(4-((6*S*,8*R*)-3-acetyl-7-isobutyl-8-methyl-6,7,8,9-tetrahydro-3H-pyrazolo[4,3-
15
16 *f*]isoquinolin-6-yl)-3,5-difluorophenyl)acrylate (1.13 g, 2.35 mmol) in IPA (20 mL) and THF (20 mL).

17
18 The mixture was stirred at 60 °C for 2 hours. The mixture was concentrated to a volume such that the
19
20 organic solvent had been removed then diluted with water (20 mL) and the aqueous layer taken to pH ~7
21
22 with 1M citric acid. The mixture was extracted into ethyl acetate (3 x 100 mL) and the combined organics
23
24 washed with brine (100 mL), dried over MgSO_4 , filtered and evaporated to give a yellow gum. The crude
25
26 product was purified by flash silica chromatography, elution gradient 0 to 10% MeOH in DCM. Pure
27
28 fractions were evaporated to dryness to afford (*E*)-3-(3,5-difluoro-4-((6*S*,8*R*)-7-isobutyl-8-methyl-6,7,8,9-
29
30 tetrahydro-3H-pyrazolo[4,3-*f*]isoquinolin-6-yl)phenyl)acrylic acid (0.810 g, 81%) as an off-white solid.

31
32 ^1H NMR (500 MHz, DMSO, 27 °C) 0.64 (d, $J = 6.5$ Hz, 3H), 0.78 (d, $J = 6.6$ Hz, 3H), 0.96 (d, $J = 6.5$
33
34 Hz, 3H), 1.65 (ddt, $J = 12.9, 6.5, 4.0$ Hz, 1H), 1.88 – 1.99 (m, 1H), 2.41 – 2.49 (m, 1H), 2.95 (dd, $J =$
35
36 16.0, 3.7 Hz, 1H), 3.25 (dd, $J = 16.0, 5.0$ Hz, 1H), 3.47 (dq, $J = 8.9, 3.3, 2.4$ Hz, 1H), 5.15 (s, 1H), 6.65
37
38 (d, $J = 16.0$ Hz, 1H), 6.69 (d, $J = 8.6$ Hz, 1H), 7.22 (d, $J = 8.6$ Hz, 1H), 7.43 (d, $J = 10.3$ Hz, 2H), 7.52 (d,
39
40 $J = 16.0$ Hz, 1H), 8.09 (d, $J = 1.0$ Hz, 1H), 12.86 (s, 2H); ^{13}C NMR (125 MHz, DMSO, 27 °C) 11.5, 20.5,
41
42 21.1, 26.3, 32.6, 48.2, 54.8, 58.2, 108.4, 111.8 (d, $J = 23.8$ Hz, 2C), 122.5, 122.7 (t, $J = 15.2$ Hz), 123.2,
43
44 125.7, 126.6, 126.7, 132.2, 136.6 (d, $J = 10.6$ Hz), 139.1, 141.7, 161.8 (d, $J = 248.5$ Hz, 2C), 167.72; ^{19}F
45
46 NMR (376 MHz, DMSO, 27 °C) -112.5; m/z : ES+ $[\text{M}+\text{H}]^+ 426$; HRMS (ESI) for $\text{C}_{24}\text{H}_{25}\text{F}_2\text{N}_3\text{O}_2$ (MH^+);
47
48 calcd, 426.1988; found, 426.1987.

49
50 **(*E*)-3-[3,5-difluoro-4-[(6*S*,8*R*)-7-(2-fluoro-2-methyl-propyl)-8-methyl-3,6,8,9-**
51
52 **tetrahydropyrazolo[4,3-*f*]isoquinolin-6-yl]phenyl]prop-2-enoic acid (9).** 2M Sodium hydroxide (66.8

1 mL, 134 mmol) was added to a solution of methyl (*E*)-3-[4-[(6*S*,8*R*)-3-acetyl-7-(2-fluoro-2-methyl-propyl)-8-methyl-8,9-dihydro-6H-pyrazolo[4,3-*f*]isoquinolin-6-yl]-3,5-difluoro-phenyl]prop-2-enoate (6.67 g, 13.4 mmol) in THF (34 mL) / methanol (34 mL). The reaction was stirred at room temperature for 16 hours. EtOAc (200 mL) and water (200 mL) were added, then the pH of the aqueous was adjusted to ~6 by addition of 2N HCl. The layers were separated, and the aqueous layer was extracted with EtOAc (2 x 200 mL). The combined organics were dried (MgSO₄) and concentrated. The crude product was purified by flash silica chromatography, elution gradient 0 to 5% MeOH in DCM. Pure fractions were evaporated to dryness to afford (*E*)-3-[3,5-difluoro-4-[(6*S*,8*R*)-7-(2-fluoro-2-methyl-propyl)-8-methyl-3,6,8,9-tetrahydropyrazolo[4,3-*f*]isoquinolin-6-yl]phenyl]prop-2-enoic acid (5.82 g, 98%) as a cream foam. ¹H NMR (500 MHz, CDCl₃, 27 °C) 0.98 (d, *J* = 6.5 Hz, 3H), 1.09 (d, *J* = 21.4 Hz, 3H), 1.16 (d, *J* = 21.5 Hz, 3H), 2.26 (dd, *J* = 27.2, 14.9 Hz, 1H), 2.91 (dd, *J* = 9.3, 5.6 Hz, 1H), 2.94 – 2.99 (m, 1H), 3.28 (dd, *J* = 16.1, 5.0 Hz, 1H), 3.62 (dq, *J* = 9.1, 3.4, 2.4 Hz, 1H), 5.22 (s, 1H), 6.62 (d, *J* = 16.1 Hz, 2H), 6.65 (d, *J* = 8.8 Hz, 1H), 7.20 (d, *J* = 8.6 Hz, 1H), 7.41 (d, *J* = 10.6 Hz, 2H), 7.50 (d, *J* = 16.0 Hz, 1H), 8.08 (d, *J* = 1.0 Hz, 1H), 12.85 (s, 2H); ¹³C NMR (125 MHz, DMSO, 27 °C) 11.1, 24.1 (d, *J* = 24.6 Hz), 25.0 (d, *J* = 24.4 Hz), 31.9, 49.3 (d, *J* = 4.2 Hz), 54.3, 57.3 (d, *J* = 21.4 Hz), 96.9 (d, *J* = 166.6 Hz), 107.9, 111.4 (d, *J* = 23.9 Hz, 2C), 121.7 (t, *J* = 15.2 Hz), 122.0, 122.6, 125.2, 125.9, 126.2, 131.8, 136.3 (t, *J* = 10.7 Hz), 138.6, 141.2, 161.4 (d, *J* = 248.6 Hz, 2C), 167.2; ¹⁹F NMR (376 MHz, DMSO, 27 °C) -137.1, -112.1; *m/z*: ES+ [M+H]⁺ 444; HRMS (ESI) for C₂₄H₂₄F₃N₃O₂ (MH⁺); calcd, 444.1893; found, 444.1889.

(*E*)-3-(4-((6*S*,8*R*)-7-(2,2-difluoropropyl)-8-methyl-6,7,8,9-tetrahydro-3H-pyrazolo[4,3-*f*]isoquinolin-6-yl)-3,5-difluorophenyl)acrylic acid (10). Aqueous sodium hydroxide (2 M, 18.69 mL, 37.38 mmol) was added slowly to a solution of methyl (*E*)-3-(4-((6*S*,8*R*)-7-(2,2-difluoropropyl)-8-methyl-6,7,8,9-tetrahydro-3H-pyrazolo[4,3-*f*]isoquinolin-6-yl)-3,5-difluorophenyl)acrylate (3.45 g, 7.48 mmol) in methanol (40 mL) and THF (20 mL). The reaction mixture was stirred at room temperature for 1 hour. The reaction mixture was diluted with water (150 mL) and adjusted to pH ~6 with aqueous HCl (2 M). The mixture was extracted with EtOAc (3 x 150 mL) and the combined organic layers were washed with saturated aqueous sodium chloride (30 mL), dried over magnesium sulfate, filtered and concentrated. The

1
2 resulting residue was purified by flash silica chromatography, elution gradient 0 to 75% EtOAc in
3
4 heptane. Product fractions were evaporated to dryness to afford (*E*)-3-(4-(((6*S*,8*R*)-7-(2,2-difluoropropyl)-
5
6 8-methyl-6,7,8,9-tetrahydro-3*H*-pyrazolo[4,3-*f*]isoquinolin-6-yl)-3,5-difluorophenyl)acrylic acid (2.45 g,
7
8 73%) as a white solid. ¹H NMR (500 MHz, CDCl₃, 27 °C) 1.04 (s, 3H), 1.42 (t, *J* = 19.1 Hz, 3H), 2.51 –
9
10 2.66 (m, 1H), 2.95 (dd, *J* = 16.3, 4.4 Hz, 1H), 3.06 – 3.19 (m, 1H), 3.21 – 3.30 (m, 1H), 3.52 (dt, *J* = 7.0,
11
12 4.9 Hz, 1H), 5.28 (s, 1H), 6.63 (d, *J* = 16.0 Hz, 1H), 6.69 (d, *J* = 8.6 Hz, 1H), 7.22 (d, *J* = 8.5 Hz, 1H),
13
14 7.43 (d, *J* = 10.7 Hz, 2H), 7.50 (d, *J* = 16.0 Hz, 1H), 8.08 (d, *J* = 1.0 Hz, 1H), 12.59 (s, 1H), 12.99 (s,
15
16 1H); ¹³C NMR (125 MHz, DMSO, 27 °C) 12.8, 21.3 (t, *J* = 26.1 Hz), 32.0, 50.2, 54.6 (t, *J* = 29.2 Hz),
17
18 55.0, 108.6, 112.0 (d, *J* = 24.1 Hz, 2C), 121.5 (t, *J* = 15.3 Hz), 122.6, 123.1, 125.4 (t, *J* = 238 Hz), 125.7,
19
20 126.1, 126.3, 132.3, 137.1 (t, *J* = 10.8 Hz), 139.1, 141.7, 161.8 (d, *J* = 248.7 Hz, 2C), 167.7; ¹⁹F NMR
21
22 (376 MHz, DMSO, 27 °C) -90.7, -90.6, -112.2; *m/z*: ES+ [M+H]⁺ 448; HRMS (ESI) for C₂₃H₂₁F₄N₃O₂
23
24 (MH⁺); calcd, 448.1643; found, 448.1643.

25
26
27
28
29 **(*E*)-3-[4-(((6*S*,8*R*)-7-(2-fluoro-2-methyl-propyl)-8-methyl-3,6,8,9-tetrahydropyrazolo[4,3-
30
31 *f*]isoquinolin-6-yl)-3-methoxy-phenyl]prop-2-enoic acid (11).** Method A: 2M sodium hydroxide
32
33 solution (2.0 mL, 4.0 mmol) was added to a solution of methyl (*E*)-3-[4-(((6*S*,8*R*)-3-acetyl-7-(2-fluoro-2-
34
35 methyl-propyl)-8-methyl-8,9-dihydro-6*H*-pyrazolo[4,3-*f*]isoquinolin-6-yl)-3-methoxy-phenyl]prop-2-
36
37 enoate (197 mg, 0.40 mmol) in THF (1.0 mL) and methanol (1.0 mL) and the reaction was stirred at
38
39 ambient temperature for 2 hours. EtOAc (10 mL) and water (10 mL) were added and the pH of the
40
41 aqueous phase was adjusted to ~6 by addition of 2N HCl solution. The layers were separated and the
42
43 aqueous phase was extracted with EtOAc (2 x 10 mL). The combined organics were dried (MgSO₄) and
44
45 concentrated. The crude product was purified by flash silica chromatography, elution gradient 25 to 100%
46
47 EtOAc in heptane. Pure fractions were evaporated to dryness to afford (*E*)-3-[4-(((6*S*,8*R*)-7-(2-fluoro-2-
48
49 methyl-propyl)-8-methyl-3,6,8,9-tetrahydropyrazolo[4,3-*f*]isoquinolin-6-yl)-3-methoxy-phenyl]prop-2-
50
51 enoic acid (115 mg, 65%) as a pale yellow solid.

52
53
54
55
56
57 Method B: 2.0 M Sodium hydroxide (23.35 mL, 46.71 mmol) was added to a solution of methyl (*E*)-3-(4-
58
59 ((6*S*,8*R*)-7-(2-fluoro-2-methylpropyl)-8-methyl-6,7,8,9-tetrahydro-3*H*-pyrazolo[4,3-*f*]isoquinolin-6-yl)-3-

1 methoxyphenyl)acrylate (2.11 g, 4.67 mmol) in THF (20 mL) / methanol (20 mL). The reaction was
2 stirred at room temperature for 2 hours. The organic solvents were removed *in vacuo* then water (100 mL)
3 was added and the pH adjusted to ~6 by addition of 2M HCl. This was then extracted with EtOAc (3 x
4 100 mL) then the combined organics were washed with brine (100 mL), dried (Na₂SO₄), filtered and
5 evaporated to an orange gum which was purified by flash silica chromatography, elution gradient 20 to
6 100% EtOAc in heptane. Pure fractions were evaporated to dryness to afford (*E*)-3-(4-((6*S*,8*R*)-7-(2-
7 fluoro-2-methylpropyl)-8-methyl-6,7,8,9-tetrahydro-3H-pyrazolo[4,3-*f*]isoquinolin-6-yl)-3-

8 methoxyphenyl)acrylic acid (1.964 g, 96%) as a yellow solid. ¹H NMR (500 MHz, DMSO, 27 °C) 0.97
9 (d, *J* = 6.5 Hz, 3H), 1.18 (d, *J* = 11.4 Hz, 3H), 1.22 (d, *J* = 11.5 Hz, 3H), 2.24 (dd, *J* = 26.5, 14.7 Hz, 1H),
10 2.74 – 2.83 (m, 1H), 2.83 – 2.89 (m, 1H), 3.22 (dd, *J* = 16.6, 5.0 Hz, 1H), 3.59 (p, *J* = 6.1 Hz, 1H), 3.92
11 (s, 3H), 5.34 (s, 1H), 6.52 (d, *J* = 16.0 Hz, 1H), 6.63 (d, *J* = 8.7 Hz, 1H), 6.86 (d, *J* = 7.9 Hz, 1H), 7.05
12 (dd, *J* = 8.0, 1.6 Hz, 1H), 7.13 – 7.20 (m, 1H), 7.35 (d, *J* = 1.6 Hz, 1H), 7.51 (d, *J* = 15.9 Hz, 1H), 8.05 (d,
13 *J* = 1.0 Hz, 1H), 12.46 (s, 1H), 12.86 (s, 1H); ¹³C NMR (125 MHz, DMSO, 27 °C) 13.1, 24.7 (d, *J* = 24.3
14 Hz), 25.5 (d, *J* = 24.6 Hz), 31.0, 47.1 (d, *J* = 3.8 Hz), 55.6, 56.0 (d, *J* = 21.9 Hz), 56.8, 97.1 (d, *J* = 165.7
15 Hz), 107.9, 110.3, 119.3, 120.3, 122.5, 126.0, 126.7, 127.9, 131.4, 131.6, 134.1, 135.2, 138.5, 143.7,
16 157.6, 167.6; ¹⁹F NMR (376 MHz, DMSO, 27 °C) -134.8; *m/z* (ES⁺), [M+H]⁺ = 438; HRMS (ESI) for
17 C₂₅H₂₈FN₃O₃ (MH⁺); calcd, 438.2188; found, 438.2189.

18 (*E*)-3-[4-[(6*S*,8*R*)-7-(2,2-difluoropropyl)-8-methyl-3,6,8,9-tetrahydropyrazolo[4,3-*f*]isoquinolin-6-
19 yl]-3-methoxy-phenyl]prop-2-enoic acid (**12**). Method A: 7.5 M sodium hydroxide (0.456 mL, 3.42
20 mmol) was added to a solution of methyl (*E*)-3-[4-[(6*S*,8*R*)-3-acetyl-7-(2,2-difluoropropyl)-8-methyl-8,9-
21 dihydro-6*H*-pyrazolo[4,3-*f*]isoquinolin-6-yl]-3-methoxy-phenyl]prop-2-enoate (0.17 g, 0.34 mmol) in
22 THF (2 mL) / methanol (2 mL). The reaction was stirred for room temperature for 2 hours. The mixture
23 was concentrated. Water (20 mL) was added, then the pH of the aqueous layer was adjusted to ~7 by
24 addition of 1N citric acid. The aqueous layer was extracted with EtOAc (3 x 100 mL) and the combined
25 organics were dried (MgSO₄) and concentrated. The crude product was purified by flash silica
26 chromatography, elution gradient 0 to 5% MeOH in DCM. Pure fractions were evaporated to dryness to

1
2 afford (*E*)-3-[4-[(6*S*,8*R*)-7-(2,2-difluoropropyl)-8-methyl-3,6,8,9-tetrahydropyrazolo[4,3-*f*]isoquinolin-6-
3
4 yl]-3-methoxy-phenyl]prop-2-enoic acid (0.108 g, 72%) as a cream solid.
5

6 **Method B:** 2 N Sodium hydroxide solution (11.94 mL, 23.87 mmol) was added slowly to a solution of
7
8 methyl (*E*)-3-(4-((6*S*,8*R*)-7-(2,2-difluoropropyl)-8-methyl-6,7,8,9-tetrahydro-3H-pyrazolo[4,3-
9
10 *f*]isoquinolin-6-yl)-3-methoxyphenyl)acrylate (2.175 g, 4.77 mmol) in methanol (15 mL) and THF (5
11
12 mL). The reaction mixture was stirred at room temperature for 1 hour. The reaction mixture was diluted
13
14 with water (15 mL) and adjusted to pH ~6 with 2M aqueous HCl. The mixture was extracted with EtOAc
15
16 (3 x 25 mL), the combined organics were washed with brine (1 x 30 mL), dried (MgSO₄), filtered and the
17
18 filtrate evaporated. The residue was purified by column chromatography eluting with 0-100%
19
20 EtOAc/Heptane to afford (*E*)-3-(4-((6*S*,8*R*)-7-(2,2-difluoropropyl)-8-methyl-6,7,8,9-tetrahydro-3H-
21
22 pyrazolo[4,3-*f*]isoquinolin-6-yl)-3-methoxyphenyl)acrylic acid (1.850 g, 88%) as a fawn coloured foam.
23
24 ¹H NMR (500 MHz, DMSO, 27 °C) 1.03 (d, *J* = 6.6 Hz, 3H), 1.55 (t, *J* = 19.2 Hz, 3H), 2.51 (d, *J* = 2.0
25
26 Hz, 1H), 2.87 (dd, *J* = 16.9, 7.0 Hz, 1H), 2.97 – 3.10 (m, 1H), 3.19 (dd, *J* = 16.9, 4.8 Hz, 1H), 3.47 (td, *J*
27
28 = 6.9, 5.0 Hz, 1H), 3.94 (s, 3H), 5.40 (s, 1H), 6.55 (d, *J* = 16.0 Hz, 1H), 6.67 (d, *J* = 8.6 Hz, 1H), 6.75 (d,
29
30 *J* = 7.9 Hz, 1H), 7.07 (dd, *J* = 8.0, 1.6 Hz, 1H), 7.22 (d, *J* = 8.6 Hz, 1H), 7.39 (d, *J* = 1.7 Hz, 1H), 7.54 (d,
31
32 *J* = 16.0 Hz, 1H), 8.08 (d, *J* = 1.0 Hz, 1H), 12.43 (s, 1H), 12.95 (s, 1H); ¹³C NMR (125 MHz, DMSO, 27
33
34 °C) 14.7, 21.1 (t, *J* = 25.9 Hz), 30.3, 47.1, 52.6 (t, *J* = 29.8 Hz), 55.6, 57.6, 108.2, 110.3, 119.3, 120.3,
35
36 122.4, 125.5 (t, *J* = 235 Hz), 126.4, 126.8, 126.9, 131.6, 131.7, 134.2, 134.4, 138.6, 143.8, 157.6, 167.6;
37
38 ¹⁹F NMR (376 MHz, DMSO, 27 °C) -88.6, -88.5; *m/z*: ES+ [M+H]⁺ 442; HRMS (ESI) for
39
40 C₂₄H₂₅F₂N₃O₃ (MH⁺); calcd, 442.1937; found, 442.1933.
41
42

43
44 **(*E*)-3-(4-((6*S*,8*R*)-7-(2,2-difluoropropyl)-8-methyl-6,7,8,9-tetrahydro-3H-pyrazolo[4,3-*f*]isoquinolin-
45
46 6-yl)-2-fluoro-3-methoxyphenyl)acrylic acid (13).** Hydrogen chloride (4 M in dioxane, 2 mL, 8.0
47
48 mmol) was added to a solution of methyl (*E*)-3-(4-((6*S*,8*R*)-7-(2,2-difluoropropyl)-8-methyl-3-
49
50 (tetrahydro-2H-pyran-2-yl)-6,7,8,9-tetrahydro-3H-pyrazolo[4,3-*f*]isoquinolin-6-yl)-2-fluoro-3-
51
52 methoxyphenyl)acrylate (64 mg, 0.11 mmol) in 1,4-dioxane (2 mL) and the resulting mixture stirred for
53
54 15 minutes and concentrated *in vacuo*. The residue was redissolved in a mixture of THF (2 mL), water (2
55
56
57
58
59
60

1 mL) and MeOH (2 mL). Lithium hydroxide monohydrate (24.1 mg, 0.57 mmol) was added and the mixture was stirred overnight. The reaction was concentrated to ~2 mL and the pH was adjusted to 5 using 1 M HCl. The aqueous layer was extracted with ethyl acetate (3 x 10 mL) and the combined organics were washed with brine, dried over sodium sulphate, filtered and concentrated *in vacuo* to give crude product which was purified by HPLC (Waters CSH C18 OBD column, 5 μ silica, 30 mm diameter, 100 mm length), using decreasingly polar mixtures of water (containing 0.1% formic acid) and MeCN as eluents. Fractions containing product were evaporated to dryness and purified further by silica gel chromatography eluting with 0-100% ethyl acetate in heptane to give (*E*)-3-(4-((6*S*,8*R*)-7-(2,2-difluoropropyl)-8-methyl-6,7,8,9-tetrahydro-3H-pyrazolo[4,3-*f*]isoquinolin-6-yl)-2-fluoro-3-methoxyphenyl)acrylic acid (2.1 mg, 4%) as a white solid. ¹H NMR (500 MHz, DMSO, 27 °C) 1.04 (d, *J* = 6.6 Hz, 3H), 1.54 (t, *J* = 19.1 Hz, 3H), 2.53 (s, 1H), 2.88 (dd, *J* = 17.0, 7.1 Hz, 1H), 3.07 (q, *J* = 14.0 Hz, 1H), 3.18 (dd, *J* = 17.1, 4.8 Hz, 1H), 3.44 (q, *J* = 6.4 Hz, 1H), 3.90 (d, *J* = 1.1 Hz, 3H), 5.30 (s, 1H), 6.50 (d, *J* = 16.1 Hz, 1H), 6.59 (d, *J* = 8.3 Hz, 1H), 6.72 (d, *J* = 8.6 Hz, 1H), 7.21 – 7.27 (m, 1H), 7.34 (dd, *J* = 8.3, 6.8 Hz, 1H), 7.59 (d, *J* = 16.1 Hz, 1H), 8.03 – 8.12 (m, 1H), 12.58 (s, 1H), 13.01 (s, 1H); ¹⁹F NMR (376 MHz, DMSO, 27 °C) -133.9, -89.6; m/z: ES+ [M+H]⁺ 460; HRMS (ESI) for C₂₄H₂₄F₃N₃O₃ (MH⁺); calcd, 460.1843; found, 460.1836.

(*E*)-3-(4-((6*S*,8*R*)-7-(2,2-difluoropropyl)-8-methyl-6,7,8,9-tetrahydro-3H-pyrazolo[4,3-*f*]isoquinolin-6-yl)-2-fluoro-5-methoxyphenyl)acrylic acid (14). Hydrogen chloride (4 M in dioxane, 2.0 mL, 8.0 mmol) was added to a solution of methyl (*E*)-3-(4-((6*S*,8*R*)-7-(2,2-difluoropropyl)-8-methyl-3-(tetrahydro-2H-pyran-2-yl)-6,7,8,9-tetrahydro-3H-pyrazolo[4,3-*f*]isoquinolin-6-yl)-2-fluoro-5-methoxyphenyl)acrylate (67 mg, 0.12 mmol) in 1,4-dioxane (2 mL) and the resulting mixture was stirred for 30 minutes and concentrated *in vacuo*. The residue was redissolved in a mixture of MeOH (2.0 mL), THF (2.0 mL) and water (2.0 mL). Lithium hydroxide monohydrate (25.2 mg, 0.60 mmol) was added and the mixture was stirred overnight. The reaction was concentrated to ~2 mL and the pH was adjusted to 5 using 1 M HCl. The aqueous layer was extracted with ethyl acetate (3 x 10 mL) and the combined organics were washed with brine, dried over sodium sulphate, filtered and concentrated *in vacuo* to give

1
2 crude product which was purified by HPLC (Waters CSH C18 OBD column, 5 μ silica, 30 mm diameter,
3
4 100 mm length), using decreasingly polar mixtures of water (containing 0.1% formic acid) and MeCN as
5
6 eluents. Fractions containing product were evaporated to dryness and purified further by silica gel
7
8 chromatography eluting with 0-100% ethyl acetate in heptane to give (*E*)-3-(4-((6*S*,8*R*)-7-(2,2-
9
10 difluoropropyl)-8-methyl-6,7,8,9-tetrahydro-3H-pyrazolo[4,3-*f*]isoquinolin-6-yl)-2-fluoro-5-
11
12 methoxyphenyl)acrylic acid (12.0 mg, 22%) as a dry film. ¹H NMR (500 MHz, DMSO, 27 °C) 1.02 (d, *J*
13
14 = 6.6 Hz, 3H), 1.55 (t, *J* = 19.1 Hz, 3H), 2.53 (s, 1H), 2.86 (dd, *J* = 16.8, 6.6 Hz, 1H), 3.04 (q, *J* = 13.8
15
16 Hz, 1H), 3.23 (dd, *J* = 17.0, 4.9 Hz, 1H), 3.46 (td, *J* = 6.7, 5.0 Hz, 1H), 3.93 (s, 3H), 5.36 (s, 1H), 6.57 (d,
17
18 *J* = 11.3 Hz, 1H), 6.67 (d, *J* = 16.1 Hz, 1H), 6.67 (d, *J* = 8.7 Hz, 1H), 7.23 (d, *J* = 8.7 Hz, 1H), 7.45 (d, *J* =
19
20 6.1 Hz, 1H), 7.57 (d, *J* = 16.1 Hz, 1H), 8.07 (s, 1H), 12.55 (s, 1H), 13.01 (s, 1H); ¹⁹F NMR (376 MHz,
21
22 DMSO, 27 °C) -126.7, -88.8; *m/z*: ES+ [M+H]⁺ 460; HRMS (ESI) for C₂₄H₂₄F₃N₃O₃ (MH⁺); calcd,
23
24 460.1843; found, 460.1845.

25
26
27
28
29 **(*E*)-3-(4-((6*S*,8*R*)-7-(2,2-difluoropropyl)-8-methyl-6,7,8,9-tetrahydro-3H-pyrazolo[4,3-*f*]isoquinolin-
30
31 6-yl)-3-fluoro-5-methoxyphenyl)acrylic acid (15).** Sodium hydroxide (2.0 M, 2.11 mL, 4.22 mmol) was
32
33 added to (*E*)-methyl 3-(4-((6*S*,8*R*)-7-(2,2-difluoropropyl)-8-methyl-6,7,8,9-tetrahydro-3H-pyrazolo[4,3-
34
35 *f*]isoquinolin-6-yl)-3-fluoro-5-methoxyphenyl)acrylate (0.20 g, 0.42 mmol) in THF (3 mL) / MeOH (3
36
37 mL). The resulting solution was stirred at 20 °C for 2 hours. The crude product was purified by ion
38
39 exchange chromatography, using an SCX column. The desired product was eluted from the column using
40
41 7M NH₃/MeOH and pure fractions were evaporated to dryness to afford (*E*)-3-(4-((6*S*,8*R*)-7-(2,2-
42
43 difluoropropyl)-8-methyl-6,7,8,9-tetrahydro-3H-pyrazolo[4,3-*f*]isoquinolin-6-yl)-3-fluoro-5-
44
45 methoxyphenyl)acrylic acid (0.176 g, 91%) as a pale yellow solid. ¹H NMR (500 MHz, DMSO, 27 °C)
46
47 1.01 (d, *J* = 6.4 Hz, 3H), 1.34 (t, *J* = 19.1 Hz, 3H), 2.50 – 2.61 (m, 1H), 2.95 (dd, *J* = 16.0, 3.2 Hz, 1H),
48
49 3.01 – 3.13 (m, 1H), 3.31 (dd, *J* = 15.9, 5.3 Hz, 1H), 3.56 (ddd, *J* = 6.6, 5.0, 3.2 Hz, 1H), 3.89 (s, 3H),
50
51 5.41 (s, 1H), 6.61 (d, *J* = 8.6 Hz, 1H), 6.63 (d, *J* = 16.0 Hz, 1H), 7.02 (d, *J* = 11.3 Hz, 1H), 7.18 (d, *J* =
52
53 8.6 Hz, 1H), 7.23 – 7.32 (m, 1H), 7.49 (d, *J* = 15.9 Hz, 1H), 8.07 (d, *J* = 1.0 Hz, 1H), 10.75 (s, br, 1H),
54
55 12.95 (s, 1H); ¹³C NMR (125 MHz, DMSO, 27 °C) 11.4, 21.1 (t, *J* = 26.2 Hz), 32.7, 50.2, 53.7, 54.7 (t, *J*
56
57
58
59
60

= 29.6 Hz), 57.0, 107.3, 108.2, 108.7, 121.8, 122.2, 123.1, 125.5, 125.6, 125.8, 127.6, 132.2, 136.5 (d, J = 11.0 Hz), 139.0, 142.4, 159.4, 162.4 (d, J = 248.7 Hz), 168.1; ^{19}F NMR (376 MHz, DMSO, 27 °C) -109.7, -89.8, -89.8; m/z : ES+ [M+H]⁺ 460; HRMS (ESI) for C₂₄H₂₄F₃N₃O₃ (MH⁺); calcd, 460.1843; found, 460.1844.

(*E*)-3-(3,5-difluoro-4-((6*S*,8*R*)-7-(2-fluoro-2-methylpropyl)-6,8-dimethyl-6,7,8,9-tetrahydro-3H-pyrazolo[4,3-*f*]isoquinolin-6-yl)phenyl)acrylic acid (16). 4N HCl in dioxane (3.26 mL, 6.52 mmol) was added to a solution of *tert*-butyl (6*S*,8*R*)-6-(4-((*E*)-3-(*tert*-butoxy)-3-oxoprop-1-en-1-yl)-2,6-difluorophenyl)-7-(2-fluoro-2-methylpropyl)-6,8-dimethyl-6,7,8,9-tetrahydro-3H-pyrazolo[4,3-*f*]isoquinoline-3-carboxylate (400 mg, 0.65 mmol) in DCM (4.24 mL) and the reaction was stirred at room temperature for 2 hours. The reaction was diluted with DCM and water, then the pH was adjusted to ~6 by addition of NaHCO₃ solution. The layers were separated, then the aqueous layer was extracted with DCM (x2). The combined organics were dried and evaporated then the crude product was purified by flash silica chromatography, elution gradient 0 to 100% EtOAc in heptane. Pure fractions were evaporated to dryness to afford (*E*)-3-(3,5-difluoro-4-((6*S*,8*R*)-7-(2-fluoro-2-methylpropyl)-6,8-dimethyl-6,7,8,9-tetrahydro-3H-pyrazolo[4,3-*f*]isoquinolin-6-yl)phenyl)acrylic acid (263 mg, 88%) as a beige solid. ^1H NMR (500 MHz, DMSO, 27 °C) 0.90 (d, J = 21.6 Hz, 3H), 1.06 (d, J = 6.7 Hz, 3H), 1.11 (d, J = 21.4 Hz, 3H), 1.82 (d, J = 4.4 Hz, 3H), 2.37 – 2.47 (m, 1H), 3.00 (dd, J = 15.6, 1.8 Hz, 1H), 3.13 (t, J = 14.3 Hz, 1H), 3.32 (q, J = 6.2 Hz, 1H), 3.75 – 3.83 (m, 1H), 6.57 (d, J = 16.0 Hz, 1H), 6.85 (d, J = 8.7 Hz, 1H), 7.20 (d, J = 8.7 Hz, 1H), 7.28 (d, J = 12.5 Hz, 2H), 7.45 (d, J = 16.0 Hz, 1H), 8.10 (d, J = 1.0 Hz, 1H), 12.78 (s, 2H); ^{13}C NMR (126 MHz, DMSO, 27 °C) 16.0, 23.1 (d, J = 24.9 Hz), 25.9 (d, J = 24.7 Hz), 26.7, 32.2, 48.4 (d, J = 6.9 Hz), 55.2 (d, J = 20.9 Hz), 62.5, 97.7 (d, J = 166.4 Hz), 107.9, 111.9 (d, J = 26.6 Hz, 2C), 121.8, 122.4, 123.8, 125.5, 125.6 (t, J = 12.4 Hz), 132.1, 133.2, 135.4 (t, J = 11.7 Hz), 138.2, 141.0, 161.5 (d, J = 249.7 Hz, 2C), 167.2; ^{19}F NMR (376 MHz, DMSO, 27 °C) -133.7, -106.3; m/z : ES+ [M+H]⁺ 458; HRMS (ESI) for C₂₅H₂₆F₃N₃O₂ (MH⁺); calcd, 458.2050; found, 458.2049.

(*E*)-3-(4-((6*S*,8*R*)-7-(2,2-difluoropropyl)-6,8-dimethyl-6,7,8,9-tetrahydro-3H-pyrazolo[4,3-*f*]isoquinolin-6-yl)-3,5-difluorophenyl)acrylic acid (17). 4N HCl in dioxane (1.78 mL, 7.12 mmol) was

1
2 added to (6*S*,8*R*)-*tert*-butyl 6-(4-((*E*)-3-(*tert*-butoxy)-3-oxoprop-1-en-1-yl)-2,6-difluorophenyl)-7-(2,2-
3 difluoropropyl)-6,8-dimethyl-6,7,8,9-tetrahydro-3H-pyrazolo[4,3-*f*]isoquinoline-3-carboxylate (220 mg,
4 0.36 mmol) and the reaction was stirred at room temperature for 3 hours. The reaction was diluted with
5 EtOAc, then the pH was adjusted to ~6 by addition of water and saturated aqueous NaHCO₃. The layers
6 were separated, then the aqueous layer was extracted with EtOAc (x2). The combined organics were
7 dried and evaporated and the crude product was purified by flash silica chromatography, elution gradient
8 0 to 100% EtOAc in heptane. Pure fractions were evaporated to dryness to afford (*E*)-3-(4-((6*S*,8*R*)-7-
9 (2,2-difluoropropyl)-6,8-dimethyl-6,7,8,9-tetrahydro-3H-pyrazolo[4,3-*f*]isoquinolin-6-yl)-3,5-
10 difluorophenyl)acrylic acid (155 mg, 94%) as a beige solid. ¹H NMR (500 MHz, DMSO, 27 °C) 1.11 (d,
11 *J* = 6.6 Hz, 3H), 1.21 (t, *J* = 19.1 Hz, 3H), 1.86 (t, *J* = 4.2 Hz, 3H), 2.78 (ddd, *J* = 22.2, 15.1, 11.0 Hz,
12 1H), 3.05 (dd, *J* = 15.7, 2.0 Hz, 1H), 3.17 – 3.27 (m, 1H), 3.30 (d, *J* = 5.9 Hz, 1H), 3.65 (dtt, *J* = 11.6, 7.4,
13 3.5 Hz, 1H), 6.60 (d, *J* = 16.0 Hz, 1H), 6.90 (d, *J* = 8.8 Hz, 1H), 7.23 (d, *J* = 8.7 Hz, 1H), 7.30 – 7.35 (m,
14 2H), 7.47 (d, *J* = 16.0 Hz, 1H), 8.12 (d, *J* = 1.0 Hz, 1H), 12.55 (s, 1H), 12.98 (s, 1H); ¹³C NMR (126
15 MHz, DMSO, 27 °C) 16.9, 21.0 (t, *J* = 25.9 Hz), 27.5, 32.6, 49.5, 52.7 (t, *J* = 32.9 Hz), 63.0, 108.6, 112.5
16 (d, *J* = 26.8 Hz, 2C), 122.4, 122.8, 124.1, 125.6 (t, *J* = 12.4 Hz), 126.0, 126.1 (t, *J* = 237 Hz), 132.7,
17 133.3, 136.2 (t, *J* = 11.9 Hz), 138.7, 141.4, 161.9 (d, *J* = 250.1 Hz, 2C), 167.6; ¹⁹F NMR (376 MHz,
18 DMSO, 27 °C) -106.4, -88.6; *m/z*: ES+ [M+H]⁺ 462; HRMS (ESI) for C₂₄H₂₃F₄N₃O₂ (MH⁺); calcd,
19 462.1799; found, 462.1797.

20
21
22
23
24
25
26
27
28
29
30
31
32
33
34
35
36
37
38
39
40
41
42
43
44
45
46
47
48
49
50
51
52
53
54
55
56
57
58
59
60
**(*E*)-3-(4-((6*S*,8*R*)-7-(2-fluoro-2-methylpropyl)-6,8-dimethyl-6,7,8,9-tetrahydro-3H-pyrazolo[4,3-
f]isoquinolin-6-yl)-3-methoxyphenyl)acrylic acid (18).** Aqueous NaOH (2N, 0.68 mL, 1.35 mmol) was
added to a solution of methyl (*E*)-3-(4-((6*S*,8*R*)-7-(2-fluoro-2-methylpropyl)-6,8-dimethyl-6,7,8,9-
tetrahydro-3H-pyrazolo[4,3-*f*]isoquinolin-6-yl)-3-methoxyphenyl)acrylate (90 mg, 0.14 mmol) in THF
(1.0 mL) and methanol (1.0 mL). The reaction was stirred at room temperature for 2 hours and then
EtOAc and water were added. The pH was adjusted to ~6 by addition of aqueous HCl (2N) and the layers
were separated. The aqueous layer was extracted with EtOAc and the organic layer was dried over
sodium sulfate, filtered and concentrated under reduced pressure. The resulting residue was purified by

1
2 flash silica chromatography, elution gradient 0 to 15% MeOH in DCM. Product fractions were
3
4 evaporated to dryness to afford (*E*)-3-(4-((6*S*,8*R*)-7-(2-fluoro-2-methylpropyl)-6,8-dimethyl-6,7,8,9-
5
6 tetrahydro-3*H*-pyrazolo[4,3-*f*]isoquinolin-6-yl)-3-methoxyphenyl)acrylic acid (31 mg, 51%) as a
7
8 colourless solid. ¹H NMR (500 MHz, DMSO, 27 °C) 0.86 (d, *J* = 21.8 Hz, 3H), 1.02 (d, *J* = 17.5 Hz, 3H),
9
10 1.04 (d, *J* = 2.7 Hz, 3H), 1.73 (s, 3H), 2.28 – 2.42 (m, 1H), 2.91 (d, *J* = 13.8 Hz, 1H), 2.97 (dd, *J* = 15.5,
11
12 2.6 Hz, 1H), 3.27 (s, 3H), 3.32 (s, 1H), 3.77 (s, 1H), 6.49 (d, *J* = 16.0 Hz, 1H), 6.66 (d, *J* = 8.7 Hz, 1H),
13
14 7.08 (d, *J* = 1.6 Hz, 1H), 7.11 (s, 1H), 7.16 (dd, *J* = 8.1, 1.7 Hz, 1H), 7.38 (s, 1H), 7.48 (d, *J* = 16.0 Hz,
15
16 1H), 8.07 (d, *J* = 1.0 Hz, 1H), 12.41 (s, 1H), 12.84 (s, 1H); ¹³C NMR (126 MHz, DMSO, 27 °C) 15.7,
17
18 23.1 (d, *J* = 25.1 Hz), 25.2, 26.1 (d, *J* = 24.8 Hz), 32.2, 47.8 (d, *J* = 6.9 Hz), 53.8, 55.1, 61.3, 98.1 (d, *J* =
19
20 166.1 Hz), 107.1, 111.7, 119.2, 119.8, 122.5, 124.8, 125.6, 128.5, 131.9, 133.2, 134.2, 138.0, 139.0,
21
22 143.5, 158.2, 167.7; ¹⁹F NMR (376 MHz, DMSO, 27 °C) -132.9; m/z: ES+ [M+H]⁺ 452; HRMS (ESI)
23
24 for C₂₆H₃₀FN₃O₃ (MH⁺); calcd, 452.2344; found, 452.2346.
25
26
27
28
29
30
31

32 **Biochemical and *in vitro* cell assays:** Binding, ER agonism, antagonism, downregulation, and cell
33
34 proliferation assays were carried out as described previously³³ with the exception that proliferation was
35
36 measured in the presence of 0.1 nM estradiol. Compounds and fulvestrant obtained from AstraZeneca
37
38 compound collection were dissolved in DMSO to a concentration of 10 mmol/L and stored under
39
40 nitrogen. Cell lines were incubated at 37 °C and 5% CO₂ in a humidified atmosphere in RPMI1640
41
42 (phenol red-free) supplemented with 5% charcoal-stripped FCS and 2 mmol/L glutamine. MCF-7 cell
43
44 line authentication date at AstraZeneca cell banking (STR fingerprinting): September 2015.
45
46
47
48
49

50 **Western blotting:** Expression levels of protein were assessed using standard Western blotting techniques
51
52 (NuPAGE Novex 4%–12% Bis-Tris gels). Cells were lysed in 25 mmol/L Tris/HCL pH 6.8, 3 mmol/L
53
54 EDTA, 3 mmol/L EGTA, 50 mmol/L NaF, 2 mmol/L sodium orthovanadate, 270 mmol/L sucrose, 10
55
56 mmol/L β-glycerophosphate, 5 mmol/L sodium pyrophosphate and 0.5% Triton X-100 supplemented
57
58 with protease inhibitors (Roche) and phosphatase inhibitors (Pierce). Antibodies to ER (SP1, Thermo) or
59
60

1
2 GAPDH (2118, CST) were diluted in 5% milk-PBS-Tween and signal detected using SuperSignal West
3
4 Dura HRP substrate followed by visualization on a Syngene ChemiGenius Imager.
5
6

7
8 **MCF-7 Xenograft Studies:** All animal studies were conducted in accordance with U.K. Home Office
9
10 legislation, the Animal Scientific Procedures Act 1986, as well as the AstraZeneca Global Bioethics
11
12 policy which are consistent with The American Chemical Society Publications rules and ethical
13
14 guidelines. All experimental work is outlined in project licence 40/3483, which has gone through the
15
16 AstraZeneca Ethical Review Process. Male CB17 SCID mice older than 5-6 weeks and weighing more
17
18 than 18 g were housed in individually vented caging systems in a 12-h light/12-h dark environment and
19
20 maintained at uniform temperature and humidity. Mice were anaesthetised with isoflurane and surgically
21
22 implanted with a 0.5 mg/21 day estrogen pellet (Innovative Research, USA) sub cutaneously. 24 hours
23
24 later MCF-7 cells (5×10^6) were implanted subcutaneously in the hind flank. Tumour growth was
25
26 calculated weekly by bilateral caliper measurement (length x width) and mice randomised into vehicle or
27
28 treatment groups of 9 animals for efficacy studies and 5 animals for PD studies, with approximate mean
29
30 start size of 0.2 to 0.4 cm³ for efficacy studies or 0.5 to 0.8 cm³ for PD studies. Group size was calculated
31
32 by a power analysis to enable statistically robust detection of tumor growth inhibition (>9 per group) or
33
34 pharmacodynamic endpoint (>5 per group). Compound **9** was formulated in vehicle (40% PEG 400
35
36 (Sigma), 30% of a 20% solution of Captosol (Ligand) and 30% water for injection) at the appropriate
37
38 concentration to dose at 10 ml/kg. Mice were dosed once daily by oral gavage at the times and doses
39
40 indicated for the duration of the treatment period. Tumour growth inhibition from start of treatment was
41
42 assessed by comparison of the mean change in tumour volume for the control and treated groups.
43
44 Statistical significance was evaluated using a one-tailed Student t test. Tumours were excised at specific
45
46 time points and fragments snap-frozen in liquid nitrogen and stored at -80 °C.
47
48
49
50
51
52
53

54
55 **Tumour protein analysis:** Tumour fragments were added to Cell Extraction buffer (Invitrogen:
56
57 FNN0011) with added Sigma Phosphatase inhibitors (No. 2 (P5726) and 3 (P0044) 1 in 100 dilution) and
58
59 Roche Complete (11836145001) protease inhibitor, 1 mM DTT and homogenised, sonicated, and
60

1
2 centrifuged before protein quantification with Bradford Reagent (Bio-Rad). Equal protein loadings were
3
4 run on Bis-Tris Criterion gels (4-12% Gels) using standard methods. Detection of PR protein is as
5
6 described in previous immunoblotting section. Vinculin protein levels were measured as a loading control
7
8 using V931 Sigma (mouse) and anti-mouse HRP-linked antibody. An unpaired two-tailed t test was used
9
10 to examine the statistical differences between the vehicle and treated groups.
11
12
13

14 **NMR stability:** The hydrolytic stability study in solution was carried out in deuterated pH 4 and 7.4
15
16 buffers at 27 °C in the absence of direct light, over a period of eight days using NMR spectroscopy and
17
18 LC-MS. Each compound from a 25 mM DMSO-*d*6 stock was diluted to a final 1 mM concentration in
19
20 each of the buffers and then transferred to an NMR tube and MS vial. The stability was followed by NMR
21
22 (500 MHz, water suppression ¹H spectra, 64 scans) and LC-MS at time points 0 h, 24 h, 72 h and 192 h (8
23
24 days). The level of degradation was derived from the ratio of integrals of the parent compound and
25
26 degradant(s), both in the NMR and LC-MS spectra.
27
28
29
30

31 32 ASSOCIATED CONTENT

33 34 Supporting Information

35
36 The Supporting Information is available free of charge on the ACS Publications website.

37
38 Experimental procedures for the synthesis of intermediates together with biological data and associated
39
40 errors, NMR conformation, crystallography and molecular formula strings (PDF)
41
42

43
44 Molecular formula strings (CSV)
45
46

47 Accession Codes

48
49 Crystal structures of ER in complex with compound **9** (6IAR). Authors will release the atomic co-
50
51 ordinates and experimental data upon article publication.
52
53
54
55
56

57 AUTHOR INFORMATION

58 59 Corresponding Author

60

1
2 *E-mail: jamie.scott@astrazeneca.com.

3
4 **ORCID**

5
6
7 James S. Scott: 0000-0002-2263-7024

8
9
10 **Author Contributions**

11
12
13 The manuscript was written through contributions of all authors. All authors have given approval to the
14 final version of the manuscript.

15
16
17 **Notes**

18
19
20 The authors declare no competing financial interest.

21
22
23 **ACKNOWLEDGMENTS**

24
25
26 The Analytical and Purification teams at AstraZeneca are thanked for their contributions. Bill McCoull is
27 thanked for his valuable contributions regarding the manuscript.

28
29
30 **ABBREVIATIONS USED**

31
32
33 AI, aromatase inhibitors; AUC, area under the curve; Cl, clearance; ER α , estrogen receptor; GSH,
34 glutathione; LLE, ligand lipophilic efficiency; MDCK, Madin-Darby Canine Kidney; n.O.e. nuclear
35 Overhauser effect; P_{app}, apparent permeability; PR, progesterone receptor; RT, room temperature; SAR,
36 structure-activity relationship; SERD, selective estrogen receptor degrader; THIQ,
37 tetrahydroisoquinoline; Vd_{ss}, steady-state volume of distribution.

38
39
40
41
42
43
44
45
46
47
48 **REFERENCES**

49
50
51 1. Ferlay, J.; Steliarova-Foucher, E.; Lortet-Tieulent, J.; Rosso, S.; Coebergh, J. W.; Comber, H.;
52 Forman, D.; Bray, F. Cancer incidence and mortality patterns in Europe: estimates for 40 countries in
53 2012. *Eur. J. Cancer.*, **2013**, *49(6)*, 1374–1403.

2. Clark, G. M.; Osborne, C. K.; McGuire, W. L. Correlations between estrogen receptor, progesterone receptor, and patient characteristics in human breast cancer. *J. Clin. Oncol.*, **1984**, *2*, 1102–1109.
3. Toy, W.; Weir, H.; Razavi, P.; Lawson, M.; Goeppert, A. U.; Mazzola, A. M.; Smith, A.; Wilson, J.; Morrow, C.; Wong, W. L.; De Stanchina, E.; Carlson, K. E.; Martin, T. S.; Uddin, S.; Li, Z.; Fanning, S.; Katzenellenbogen, J. A.; Greene, G.; Baselga, J.; Chandarlapaty, S. Activating ESR1 mutations differentially affect the efficacy of ER antagonists. *Cancer Discov.*, **2017**, *7*(3), 277–287.
4. McDonnell, D. P. and Wardell, S. E. The molecular mechanisms underlying the pharmacological actions of ER modulators: Implications for new drug discovery in breast cancer. *Curr. Opin. Pharmacol.*, **2010**, *10*(6), 620–628.
5. Robertson, J. F., Fulvestrant (Faslodex) - how to make a good drug better. *Oncologist*, **2007**, *12*, 774–784.
6. Willson, T. M.; Henke, B. R.; Momtahan, T. M.; Charifson, P. S.; Batchelor, K. W.; Lubahn, D. B.; Moore, L. B.; Oliver, B. B.; Sauls, H. R., 3-4-(1,2-Diphenylbut-1-enyl)phenyl]acrylic Acid: a non-steroidal estrogen with functional selectivity for bone over uterus in rats. *J. Med. Chem.*, **1994**, *37*(11), 1550–1552.
7. (a) Lai, A.; Kahraman, M.; Govek, S.; Nagasawa, J.; Bonnefous, C.; Julien, J.; Douglas, K.; Sensintaffar, J.; Lu, N.; Lee, K.-j.; Aparicio, A.; Kaufman, J.; Qian, J.; Shao, G.; Prudente, R.; Moon, M. J.; Joseph, J. D.; Darimont, B.; Brigham, D.; Grillot, K.; Heyman, R.; Rix, P. J.; Hager, J. H.; Smith, N. D. Identification of GDC-0810 (ARN-810), an orally bioavailable selective estrogen receptor degrader (SERD) that demonstrates robust activity in Tamoxifen-resistant breast cancer xenografts. *J. Med. Chem.*, **2015**, *58*(12), 4888–4904; (b) Govek, S. P.; Nagasawa, J. Y.; Douglas, K. L.; Lai, A. G.; Kahraman, M.; Bonnefous, C.; Aparicio, A. M.; Darimont, B. D.; Grillot, K. L.; Joseph, J. D.; Kaufman, J. A.; Lee, K.-J.; Lu, N.; Moon, M. J.; Prudente, R. Y.; Sensintaffar, J.; Rix, P. J.; Hager, J. H.; Smith, N. D., Optimization of an indazole series of selective estrogen receptor degraders: tumor regression in a tamoxifen-resistant breast cancer xenograft. *Bioorg. Med. Chem. Lett.*, **2015**, *25*(22), 5163-5167.

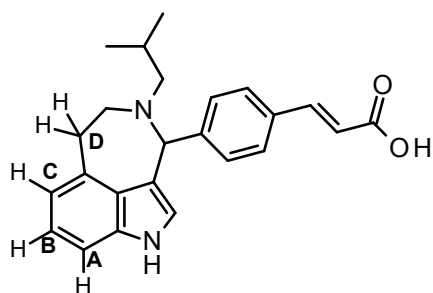
- 1
2 8. De Savi, C.; Bradbury, R. H.; Rabow, A. A.; Norman, R. A.; de Almeida, C.; Andrews, D. M.;
3
4 Ballard, P.; Buttar, D.; Callis, R. J.; Currie, G. S.; Curwen, J. O.; Davies, C. D.; Donald, C. S.; Feron, L. J.
5
6 L.; Gingell, H.; Glossop, S. C.; Hayter, B. R.; Hussain, S.; Karoutchi, G.; Lamont, S. G.; MacFaul, P.;
7
8 Moss, T. A.; Pearson, S. E.; Tonge, M.; Walker, G. E.; Weir, H. M.; Wilson, Z. Optimization of a novel
9
10 binding motif to (*E*)-3-(3,5-difluoro-4-((1*R*,3*R*)-2-(2-fluoro-2-methylpropyl)-3-methyl-2,3,4,9-tetrahydro-
11
12 1*H*-pyrido[3,4-*b*]indol-1-yl)phenyl)acrylic acid (AZD9496), a potent and orally bioavailable selective
13
14 estrogen receptor downregulator and antagonist. *J. Med. Chem.*, **2015**, *58*(20), 8128–8140.
15
16
17
18 9. Tria, G. S.; Abrams, T.; Baird, J.; Burks, H. E.; Firestone, B.; Gaither, L. A.; Hamann, L. G.; He,
19
20 G.; Kirby, C. A.; Kim, S.; Lombardo, F.; Macchi, K. J.; McDonnell, D. P.; Mishina, Y.; Norris, J. D.;
21
22 Nunez, J.; Springer, C.; Sun, Y.; Thomsen, N. M.; Wang, C.; Wang, J.; Yu, B.; Tiong-Yip, C.-L.;
23
24 Peukert, S., Discovery of LSZ102, a potent, orally bioavailable selective estrogen receptor degrader
25
26 (SERD) for the treatment of estrogen receptor positive breast cancer. *J. Med. Chem.*, **2018**, *61*(7),
27
28 2837–2864.
29
30
31
32 10. Degorce, S. L.; Bailey, A.; Callis, R.; De Savi, C.; Ducray, R.; Lamont, G.; MacFaul, P. A.;
33
34 Maudet, M.; Martin, S.; Morgentin, R.; Norman, R. A.; Peru, A.; Pink, J.; Plé, P.; Roberts, B.; Scott, J. S.
35
36 Investigation of (*E*)-3-[4-(2-oxo-3-aryl-chromen-4-yl)oxyphenyl]acrylic acids as oral selective estrogen
37
38 receptor down-regulators. *J. Med. Chem.*, **2015**, *58*(8), 3522–3533.
39
40
41
42 11. Scott, J. S.; Bailey, A.; Davies, R. D. M.; Degorce, S. L.; MacFaul, P. A.; Gingell, H.; Moss, T.;
43
44 Norman, R. A.; Pink, J. H.; Rabow, A. A.; Roberts, B.; Smith, P. D., Tetrahydroisoquinoline phenols:
45
46 selective estrogen receptor downregulator antagonists with oral bioavailability in rat. *ACS Med. Chem.*
47
48 *Lett.*, **2016**, *7*(1), 94–99.
49
50
51 12. Hoekstra, W. J.; Patel, H. S.; Liang, X.; Blanc, J.-B. E.; Heyer, D. O.; Willson, T. M.; Iannone, M.
52
53 A.; Kadwell, S. H.; Miller, L. A.; Pearce, K. H.; Simmons, C. A.; Shearin, J., Discovery of novel
54
55 quinoline-based estrogen receptor ligands using peptide interaction profiling. *J. Med. Chem.*, **2005**, *48*(6),
56
57 2243–2247.
58
59
60

- 1
2 13. Burks, H. E.; Abrams, T.; Kirby, C. A.; Baird, J.; Fekete, A.; Hamann, L. G.; Kim, S.; Lombardo,
3
4 F.; Loo, A.; Lubicka, D.; Macchi, K.; McDonnell, D. P.; Mishina, Y.; Norris, J. D.; Nunez, J.; Saran, C.;
5
6 Sun, Y.; Thomsen, N. M.; Wang, C.; Wang, J.; Peukert, S., Discovery of an acrylic acid based
7
8 tetrahydroisoquinoline as an orally bioavailable selective estrogen receptor degrader for ER α + breast
9
10 cancer. *J. Med. Chem.*, **2017**, *60*(7), 2790–2818.
- 11
12
13 14. O'Boyle, N. M.; Barrett, I.; Greene, L. M.; Carr, M.; Fayne, D.; Twamley, B.; Knox, A. J. S.;
14
15 Keely, N. O.; Zisterer, D. M.; Meegan, M. J., Lead optimization of benzoxepin-type selective estrogen
16
17 receptor (ER) modulators and downregulators with subtype-specific ER α and ER β activity. *J. Med.*
18
19 *Chem.*, **2018**, *61*(2), 514–534.
- 20
21
22 23. Suzuki, N.; Liu, X.; Laxmi, Y. R. S.; Okamoto, K.; Kim, H. J.; Zhang, G.; Chen, J. J.; Okamoto,
24
25 Y.; Shibutani, S., Anti-breast cancer potential of SS5020, a novel benzopyran antiestrogen. *Int. J.*
26
27 *Pharmacol.*, **2010**, *128*(4), 974–982.
- 28
29
30 31. Laxmi, Y. R. S.; Liu, X.; Suzuki, N.; Kim, S. Y.; Okamoto, K.; Kim, H. J.; Zhang, G.; Chen, J. J.;
32
33 Okamoto, Y.; Shibutani, S., Anti-breast cancer potential of SS1020, a novel antiestrogen lacking
34
35 estrogenic and genotoxic actions. *Int. J. Cancer*, **2010**, *127*(7), 1718–1726.
- 36
37
38 39. Xiong, R.; Zhao, J.; Gutgesell, L. M.; Wang, Y.; Lee, S.; Karumudi, B.; Zhao, H.; Lu, Y.; Tonetti,
39
40 D. A.; Thatcher, G. R. J., Novel selective estrogen receptor downregulators (SERDs) developed against
41
42 treatment-resistant breast cancer. *J. Med. Chem.*, **2017**, *60*(4), 1325–1342.
- 43
44
45 46. Kieser, K. J.; Kim, D. W.; Carlson, K. E.; Katzenellenbogen, B. S.; Katzenellenbogen, J. A.,
46
47 Characterization of the pharmacophore properties of novel selective estrogen receptor downregulators
48
49 (SERDs). *J. Med. Chem.*, **2010**, *53*(8), 3320–3329.
- 50
51
52 53. Min, J.; Guillen, V. S.; Sharma, A.; Zhao, Y.; Ziegler, Y.; Gong, P.; Mayne, C. G.; Srinivasan, S.;
53
54 Kim, S. H.; Carlson, K. E.; Nettles, K. W.; Katzenellenbogen, B. S.; Katzenellenbogen, J. A., Adamantyl
55
56 antiestrogens with novel side chains reveal a spectrum of activities in suppressing estrogen receptor
57
58 mediated activities in breast cancer cells. *J. Med. Chem.*, **2017**, *60*(14), 6321–6336.
- 59
60

- 1
2 20. Liu, J.; Zheng, S.; Guo, S.; Zhang, C.; Zhong, Q.; Zhang, Q.; Ma, P.; Skripnikova, E. V.; Bratton,
3 M. R.; Wiese, T. E.; Wang, G., Rational design of a boron-modified triphenylethylene (GLL398) as an
4 oral selective estrogen receptor downregulator. *ACS Med. Chem. Lett.*, **2017**, *8*(1), 102–106.
5
6
7
8
9 21. Garner, F.; Shomali, M.; Paquin, D.; Lyttle, C. R.; Hattersley, G. RAD1901: a novel, orally
10 bioavailable selective estrogen receptor degrader that demonstrates antitumor activity in breast cancer
11 xenograft models. *Anti-Cancer Drugs*. **2015**, *26*(9), 948–956.
12
13
14
15
16 22. (a) Nagasawa, J.; Govek, S.; Kahraman, M.; Lai, A.; Bonnefous, C.; Douglas, K.; Sensintaffar, J.;
17 Lu, N.; Lee, K.; Aparicio, A.; Kaufman, J.; Qian, J.; Shao, G.; Prudente, R.; Joseph, J. D.; Darimond, B.;
18 Brigham, D.; Maheu, K.; Heyman, R.; Rix, P.; Hager, J. H.; Smith, N. D., Identification of an orally
19 bioavailable chromene-based selective estrogen receptor degrader (SERD) that demonstrates robust
20 activity in a model of tamoxifen-resistant breast cancer. *J. Med. Chem.*, **2018**, *61*(17), 7917–7928; (b)
21 Kahraman, M.; Govek, S. P.; Nagasawa, J. Y.; Lai, A.; Bonnefous, C.; Douglas, K.; Sensintaffar, J.; Liu,
22 N.; Lee, K.; Aparicio, A.; Kaufman, J.; Qian, J.; Shao, G.; Prudente, R.; Joseph, J. D.; Darimont, B.;
23 Brigham, D.; Heyman, R.; Rix, P. J.; Hager, J. H.; Smith, N. D., Maximizing ER- α degradation
24 maximizes activity in a tamoxifen-resistant breast cancer model: identification of GDC-0927. *ACS Med.*
25 *Chem. Lett.*, **2018**, *10*(1), 50–55.
26
27
28
29
30
31
32
33
34
35
36
37
38
39 23. GSH trapping was assessed in human liver microsomes with trapping reported as a ratio to a
40 positive control, clozapine, as detailed in; Lenz, E. M.; Martin, S.; Schmidt, R.; Morin, P.-E.; Smith, R.;
41 Weston D. J.; Bayrakdarian, M., Reactive metabolite trapping screens and potential pitfalls: bioactivation
42 of a homomorpholine and formation of an unstable thiazolidine adduct. *Chem. Res. Tox.*, **2014**, *27*,
43 968–980. For the phenols examined in this assay, the most common adduct seen corresponded to a mass
44 of GSH +16. This is consistent with an epoxidation of the electron rich phenol ring, followed by ring
45 opening by GSH. While this mechanism was not confirmed with definitive structural elucidation, SAR
46 observations are consistent with this hypothesis.
47
48
49
50
51
52
53
54
55
56
57 24. Following completion of this work, a patent application (Yu, S.; Yang, F.; Chen, L.; Yan, J.;
58 Zhang, X.; Xie, Z; Chen, L.; He, M. Piperidine derivative and preparation method and pharmaceutical use
59
60

thereof. Patent application WO2016202161, December 22, 2016) from Shanghai Hengrui Pharmaceutical containing 103 examples was published. Of the many scaffolds explored, four examples contained racemic versions of the tricyclic indazole core (Ex 92, 101, 102, 103) and one was synthesised racemically and separated into constituent enantiomers (Ex 94, 95) using a different synthetic route to that described herein.

25. The assignment of this structure was based on multidimensional NMR experiments (COSY, ^{13}C HSQC, ^{13}C HMBC and ROESY). The 7-membered ring connectivity was established due to several key NMR correlations that would not be possible in the six-membered one, specifically; (a) Three aromatic protons coupled to each other in the indole ring (H_A , H_B and H_C); (b) Strong cross peak in the HMBC between H_C and C_D ; (c) Strong n.O.e peaks between H_C and H_D



26. Davies, R. D. M.; Pink, J. H.; Scott, J. S.; Bailey, A., Synthesis of 8-substituted-6-phenyl-6,7,8,9-tetrahydro-3H-pyrazolo[4,3-*f*]isoquinolines using Pictet-Spengler and Bischler-Napieralski cyclisation methods. *Tetrahedron Lett.*, **2018**, *59*(30), 2917–2920.

27. Bailey, A.; Lister A. S.; Moss, T. A.; Scott, J. S.; Wu, Y.; Lamont, S. G. Synthesis of trans 8-substituted-6-phenyl-6,7,8,9-tetrahydro-3H-pyrazolo[4,3-*f*]isoquinolines using a Pictet-Spengler approach. *Tetrahedron Lett.*, **2018**, *59*(51), 4509–4513.

28. The configuration of the stereocenter of **4** was assigned as (1*R*) based on the X-ray crystal structure of **4** in complex with the protein. The enantiomeric compound *ent-4* showed lower activity in both the binding (pIC_{50} 5.9) and downregulation (pIC_{50} 6.2) assay.

1
2 29. The configuration of the stereocenter of **6** was assigned as (1*R*) based on analogy with **2**. The
3
4 enantiomeric compound *ent*-**6** showed lower activity in both the binding (pIC₅₀ 5.8) and downregulation
5
6 (pIC₅₀ 6.2) assay.
7

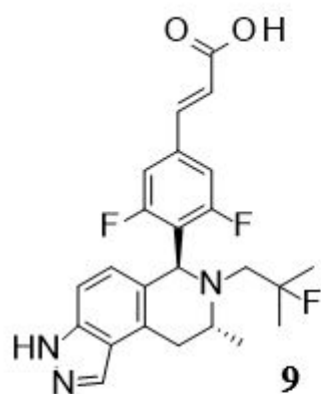
8
9 30. The switch from monomethyl to gem dimethyl in the THIQ series consistently lowered human
10
11 hepatocyte CL_{int} (e.g. cpd **12** to **14a** in ref 10 was representative of the wider series). In the indazole
12
13 series, the opposite observation was made in all matched pairs tested (e.g. cpd **6** to **5** resulting in increased
14
15 turnover was representative of the wider series) highlighting subtle differences between the series.
16

17
18 31. Of the 23 indazole compounds of this chemotype tested as part of this program, none showed any
19
20 trapping in the GSH assay (ratios all <0.04). Although the THIQ phenol matched pair of cpd **1** (cpd **10a**
21
22 in ref 10) had no detectable ratio, 35/38 other phenols looked at showed some degree of trapping.
23
24 Specifically; the phenol matched pair of cpd **2** (cpd **13** in ref 10), **3** (cpd **12** in ref 10) and **6** (cpd **23** in ref
25
26 10) had ratios of 0.16, 0.66 and 0.43 respectively.
27

28
29 32. Weir, H. M.; Bradbury, R. H.; Lawson, M.; Rabow, A. A.; Buttar, B.; Callis, R. J.; Curwen, J. O.;
30
31 de Almeida, C.; Ballard, P.; Hulse, M.; Donald, C. S.; Feron, L. J.; Karoutchi, G.; MacFaul, P.; Moss, T.;
32
33 Norman, R. A.; Pearson, S. E.; Tonge, M.; Davies, G.; Walker, G. E.; Wilson, Z.; Rowlinson, R.; Powell,
34
35 S.; Sadler, C.; Richmond, G.; Ladd, B.; Pazolli, E.; Mazzola, A. M.; D'Cruz, C.; De Savi, C., AZD9496:
36
37 an oral estrogen receptor inhibitor that blocks the growth of ER-positive and ESR1-mutant breast tumors
38
39 in preclinical models. *Cancer Res.* **2016**, *76(11)*, 3307–3318.
40
41

42
43 33. Callis, R.; Rabow, A.; Tonge, M.; Bradbury, R.; Challinor, M., Roberts, K., Jones, K.; Walker, G.
44
45 A screening assay cascade to identify and characterize novel selective estrogen receptor downregulators
46
47 (SERDs). *J. Biomol. Screen.* **2015**, *20*, 748–759.
48
49
50
51
52
53
54
55
56
57
58
59
60

GRAPHICAL ABSTRACT



ER α pIC₅₀ 9.5
logD_{7.4} 2.6
LLE 6.9
MoA degrader/antagonist

